**Steel and Composite Structures**, *Vol. 26, No. 6 (2018) 673-691*
DOI: https://doi.org/10.12989/scs.2018.26.6.673


# Nonlinear forced vibration of FG-CNTs-reinforced curved microbeam based on strain gradient theory considering out-of-plane motion

Farshid Allahkarami [1], Mansour Nikkhah-bahrami [*1] and Maryam Ghassabzadeh Saryazdi [2]

[1] *Department of Mechanical and Aerospace Engineering, Science and Research Branch, Islamic Azad University, Tehran, Iran*
[2] *Vehicle Technology Research Institute, Amirkabir University of Technology, Tehran, Iran*

(*Received September 14, 2017, Revised January 1, 2018, Accepted January 6, 2018*)

**Abstract.** The main goal of this research is to examine the in-plane and out-of-plane forced vibration of a curved nanocomposite microbeam. The in-plane and out-of-plane displacements of the structure are considered based on the first order shear deformation theory (FSDT). The curved microbeam is reinforced by functionally graded carbon nanotubes (FG-CNTs) and thus the extended rule of mixture is employed to estimate the effective material properties of the structure. Also, the small scale effect is captured using the strain gradient theory. The structure is rested on a nonlinear orthotropic viscoelastic foundation and is subjected to concentrated transverse harmonic external force, thermal and magnetic loads. The derivation of the governing equations is performed using energy method and Hamilton's principle. Differential quadrature (DQ) method along with integral quadrature (IQ) and Newmark methods are employed to solve the problem. The effect of various parameters such as volume fraction and distribution type of CNTs, boundary conditions, elastic foundation, temperature changes, material length scale parameters, magnetic field, central angle and width to thickness ratio are studied on the frequency and force responses of the structure. The results indicate that the highest frequency and lowest vibration amplitude belongs to FGX distribution type while the inverse condition is observed for FGO distribution type. In addition, the hardening-type response of the structure with FGX distribution type is more intense with respect to the other distribution types.

**Keywords:** forced vibration; curved nanocomposite microbeam; strain gradient theory; viscoelastic foundation; DQ-IQ-Newmark method

## 1. Introduction

The growing applications of small-scale structures like microbeams in micro-electro-mechanical systems (MEMS) and nano-electro-mechanical systems (NEMS) are the reason of the many theoretical and experimental investigations on the behavior of such structures.

An investigation into the response of a resonant microbeam to an electric actuation was presented by Younis and Nayfeh (2003). The improved macromodel of the fixed-fixed microbeam-based MEMS capacitive switch was presented by He *et al*. (2009) to investigate the behavior of electrically actuated MEMS capacitive switch. A nonlinear model was used to account for the mid-plane stretching, a DC electrostatic force, and an AC harmonic force. Krylov *et al*. (2011) investigated the feasibility of two-directional switching of initially curved or pre-buckled electrostatically actuated microbeams using a single electrode fabricated from the same structural layer. The dynamic response of parametrically excited microbeam arrays was governed by Gutschmidt and Gottlieb (2012) using nonlinear effects which directly influence their performance. To date, most widely used theoretical approaches, although opposite extremes with respect to complexity, were nonlinear lumped-mass and finite-element models. Ghayesh *et al*. (2017) used Timoshenko beam theory and modified couple stress theory (MCST) to investigate the nonlinear forced vibrations of a functionally graded (FG) microbeam. Rezaei and Zamanian (2017) performed a two-dimensional vibration analysis of piezoelectrically actuated microbeam. They modeled the structure based on Euler-Bernoulli beam theory and considered the effect of geometric nonlinearity. Dai *et al*. (2015) explored the nonlinear dynamics behavior of cantilevered microbeams on the basis of MCST. They derived the governing equations using Hamilton's principle and solved them employing Galerkin method. Jahangiri *et al*. (2015) investigated mechanical behavior of the functional gradient materials (FGM) micro-gripper under thermal load and DC voltage numerically taking into account the effect of intermolecular forces. Bataineh and Younis (2015) presented an investigation into the static and dynamic behavior of an electrostatically actuated clamped–clamped polysilicon microbeam resonator accounting for its fabrication imperfections. Free flexural vibration of geometrically imperfect FG microbeams is probed by Dehrouyesh-Semnani *et al*. (2016). They assumed that the mechanical properties of the FG microbeam vary through the thickness direction based on a power-law distribution. They also considered the size effect employing MCST. Ghayesh and Farokhi (2017), Peng *et al*. (2017), Dehrouyesh-Semnani *et al*. (2015) and Shafiei *et al*. (2016) are the other authors who employed MCST to study the size

*Corresponding author, Professor,
E-mail: mbahrami@ut.ac.ir



ISSN: 1229-9367 (Print), 1598-6233 (Online)

effect phenomenon in the microstructures. Erfani and Akrami (2016) studied evaluation of cyclic fracture in perforated beams using micromechanical fatigue model. Aya and Tufekci (2017) investigated the out-of-plane static behavior of curved nanobeams. They presented an exact analytical solution using initial value method. Pan *et al*. (2017) studied out-of-plane bending stiffness of carbon nanotube films on the basis of energy analysis. They validated their results by finite element simulations. Furthermore, Jafari-Talookolaei *et al*. (2017) investigated the in-plane and out-of-plane vibration modes of thin-to-moderately thick laminated composite beams with arbitrary lay-ups. They used first order shear deformation theory (FSDT) to develop the mathematical model. Also, Liu et al. (2017), Rostami *et al*. (2016) and Wang *et al*. (2016) investigated in-plane vibration of various structures. Vibration of an embedded nanocomposite curved microbeam was investigated by Allahkarami and Nikkhah-Bahrami (2017) based on the modified couple stress theory and Timoshenko beam model. In another work, Allahkarami *et al*. (2017) studied dynamic buckling analysis of an embedded curved microbeam reinforced by functionally graded carbon nanotubes. Atcı and Bağdatlı (2017a) presented the effects of non-ideal boundary conditions (BCs) on fundamental parametric resonance behavior of fluid conveying clamped microbeams. In another work by Atcı and Bağdatlı (2017b), vibration analysis of fluid conveying microbeams under non-ideal boundary conditions (BCs) was performed.

For the first time, the in-plane and out-of-plane forced vibration of a curved nanocomposite microbeam is studied in the present research. Therefore, the results of this work are of great importance in MEMS and NEMS. The FG-CNTs reinforced curved microbeam is modeled by FSDT and the material properties of the structure are estimated using the extended rule of mixture. Also, the small scale effect is considered using strain gradient theory. The structure is rested on a nonlinear orthotropic viscoelastic foundation and is subjected to concentrated transverse harmonic external force, thermal and magnetic loads. Differential quadrature (DQ) method along with integral quadrature (IQ) and Newmark methods are used to solve the problem and study the effect of various parameters on the frequency responses and force responses of the structure.

## 2. Theoretical model of problem

Fig. 1(a) represents a schematic view of a FG-CNTs reinforced curved microbeam with the length of $L$, radius of $R$ and thickness of $h$. The structure is rested on an orthotropic viscoelastic foundation which is modeled with linear and nonlinear spring, damper and orthotropic shear elements. Furthermore, four various CNTs distribution types are shown in Fig. 1(b) which are including UD, FGA, FGO and FGX.

### 2.1 Displacement field

The displacement field components of an arbitrary point

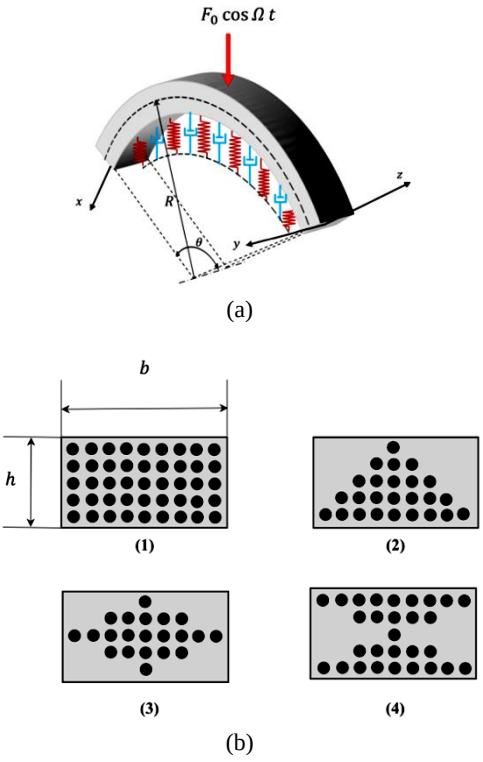


Fig. 1 (a) A schematic of FG-CNTs reinforced curved microbeam; (b) different distribution of CNTs (1) UD; (2) FGA; (3) FGO; (4) FGX

within the curved microbeam are expressed based on FSDT as follows

$$\begin{aligned} u_x(x,y,z,t) &= u(x,y,t) + z\,\varphi_x(x,y,t), \\ u_y(x,y,z,t) &= v(x,y,t) + z\,\varphi_y(x,y,t) + x\,\varphi_z(x,y,t), \\ u_z(x,y,z,t) &= w(x,y,t) - x\,\varphi_x(x,y,t), \end{aligned} \tag{1}$$

in which $u(x, y, t)$, $v(x, y, t)$ and $w(x, y, t)$ denote the displacement components of the middle surface (i.e., at $z = 0$) in direction of the x, y- and z-axis, respectively. Moreover, $\varphi_x(x, y, t)$, $\varphi_y(x, y, t)$ and $\varphi_z(x, y, t)$ indicate the rotation of the cross section of the curved microbeam around the $x$, $y$- and $z$-direction, respectively.

### 2.2 Kinematic relations

Considering Eq. (1) and nonlinear term of axial strain, we have

$$\varepsilon_{xx} = \frac{\partial u}{\partial x} + \frac{w}{R} + z\,\frac{\partial \varphi_y}{\partial x} + y\left(\frac{\varphi_x}{R} - \frac{\partial \varphi_z}{\partial x}\right) + \frac{1}{2}\left(\frac{\partial v}{\partial x}\right)^2 + \frac{1}{2}\left(\frac{\partial w}{\partial x}\right)^2 \tag{2a}$$

$$\varepsilon_{xy} = \frac{1}{2}\left(\frac{\partial v}{\partial x} - z\,\frac{\partial \varphi_x}{\partial x} - \varphi_z\right) \tag{2b}$$

$$\varepsilon_{xz} = \frac{1}{2}\left(\frac{\partial w}{\partial x} - \frac{u}{R} + y\left(\frac{\varphi_z}{R} - \frac{\partial \varphi_x}{\partial x}\right) + \left(1 - \frac{z}{R}\right)\varphi_y\right) \tag{2c}$$

### *2.3 Extended rule of mixture*

The effective material properties of the CNTs reinforced composite curved microbeam are estimated using extended rule of mixture. So, the CNTs are considered as short fibers which are aligned and straight. Thus, the effective Young's modulus and shear modulus of the CNTs reinforced composite curved beam can be obtained as (Shen 2009)

$$E_{11} = \eta_1 V_{CNT} E_{r11} + (1 - V_{CNT}) E_{11}^{m}, \tag{3}$$

$$\frac{\eta_2}{E_{22}} = \frac{V_{CNT}}{E_{r22}} + \frac{(1 - V_{CNT})}{E_{22}^{m}}, \tag{4}$$

$$\frac{\eta_3}{G_{12}} = \frac{V_{CNT}}{G_{r12}} + \frac{(1 - V_{CNT})}{G_{12}^{m}}, \tag{5}$$

where $E_{r11}$, $E_{r22}$ and $G_{r12}$ represent Young's and shear moduli of CNTs, respectively. Also, $E_m$ and $G_m$ are the mechanical properties of the matrix material, and $V_{CNT}$ indicates the volume fraction of CNTs. Furthermore, $\eta_i$ ($i$ = 1, 2, 3) indicates the CNTs efficiency parameters. In present research, four various CNTs distribution types through the thickness direction of composite curved beam are considered, comprising the uniform (UD) and functionally graded (FG) distributions which can be expresses as

$$UD: \quad V_{CNT} = V_{CNT}^{*}, \tag{6}$$

$$FGV: \; V_{CNT}(z) = \left(1 - \frac{2z}{h}\right) V_{CNT}^{*}, \tag{7}$$

$$FGO: \; V_{CNT}(z) = 2\left(1 - \frac{2|z|}{h}\right) V_{CNT}^{*}, \tag{8}$$

$$FGX: \; V_{CNT}(z) = 2\left(\frac{2|z|}{h}\right) V_{CNT}^{*}, \tag{9}$$

where

$$V_{CNT}^{*} = \frac{w_{CNT}}{w_{CNT} + (\rho_{CNT} / \rho_m) - (\rho_{CNT} / \rho_m) w_{CNT}}, \tag{10}$$

In which $w_{CNT}$ denotes the mass fraction of CNTs. Also, $\rho_m$ and $\rho_{CNT}$ represent the mass densities of matrix and CNTs, respectively. In a similar manner, the effective thermal expansion coefficients and mass density of the CNTs reinforced composite microbeam can be obtained by the following relations

$$\begin{aligned} \alpha_{xx}^{(c)} &= V_{CNT}\alpha_{r11} + (1 - V_{CNT})\alpha_m, \\ \alpha_{yy}^{(c)} &= (1 + \nu_{r12}) V_{CNT}\alpha_{r22} + (1 + \nu_m) \\ &(1 - V_{CNT})\alpha_m - \nu_{12}\alpha_{11}, \end{aligned} \tag{11}$$

$$\rho^{(c)} = V_{CNT}\rho_r + (1 - V_{CNT})\rho_m, \tag{12}$$

where $\alpha_{r11}$ and $\alpha_{r22}$ denote the thermal expansion coefficients of CNTs in the longitudinal and transverse directions, respectively. Furthermore, $\rho_m$ and $\rho_r$ indicate the mass densities of matrix and CNTs, respectively. It should be noted that the Poisson's ratio is assumed to be constant along the thickness direction.

## 3. Derivation of motion equations

The governing equations of the structure are derived using Hamilton's principle which can be expressed as

$$\int_0^t (\delta U - (\delta K + \delta W))dt = 0. \tag{13}$$

in which $U$, $K$ and $W$ indicate the total potential strain energy, total kinetic energy and work done by external forces, respectively.

The total potential energy of the structure is considered based on SGT as follows

$$U = \frac{1}{2}\int_V (\sigma_{ij}\varepsilon_{ij} + p_i\gamma_i + \tau_{ijk}^{(1)}\eta_{ijk}^{(1)} + m_{ij}^{s}\chi_{ij}^{s})dV, \tag{14}$$

in which $\varepsilon_{ij}$, $\gamma_i$, $\eta_{ijk}^{(1)}$ and $\chi_{ij}$ denote the strain tensor, the dilatation gradient vector, the deviatoric stretch gradient and the symmetric rotation gradient tensors, respectively. Based on Eq. (14), SGT is capable to consider three independent material length scale parameters and expresses the potential energy as a function of the symmetric strain tensor, the dilatation gradient vector, the deviatoric stretch gradient tensor and the symmetric rotation gradient tensor which can be considered as follows (Zhang *et al*. 2013)

$$\gamma_i = \varepsilon_{mm,i}, \tag{15a}$$

$$\begin{aligned} \eta_{ijk} &= \frac{1}{3}(\varepsilon_{jk,i} + \varepsilon_{ki,j} + \varepsilon_{ij,k}) - \frac{1}{15}\delta_{ij}(\varepsilon_{mm,k} + 2\varepsilon_{mk,m}) \\ &- \frac{1}{15}\left[\delta_{jk}(\varepsilon_{mm,i} + 2\varepsilon_{mi,m}) + \delta_{ki}(\varepsilon_{mm,j} + 2\varepsilon_{mj,m})\right], \end{aligned} \tag{15b}$$

$$\chi_{ij}^{s} = \frac{1}{2}(\theta_{i,j} + \theta_{j,i}), \tag{15c}$$

in which $u_i$ and $\delta_{ij}$ denote the displacement vector and the knocker delta, respectively. Also, the rotation vector ($\theta_i$) can be expressed as

$$\theta_i = \left(\frac{1}{2}curl(u)\right)_i. \tag{16}$$

The classical stress tensor, $\sigma_{ij}$, the higher-order stresses, $p_i$, $\tau_{ijk}^{(1)}$ and $m_{ij}$ which mentioned in Eq. (14) can be expressed as

$$\sigma_{ij} = \lambda tr\varepsilon\delta_{ij} + 2\mu\varepsilon_{ij}, \tag{17a}$$

$$p_i = 2\mu l_0^2 \gamma_i, \tag{17b}$$

$$\tau^1_{ijk} = 2\mu l_1^2 \eta^1_{ijk}, \tag{17c}$$

$$m^s_{ij} = 2\mu l_2^2 \chi^s_{ij}, \tag{17d}$$

in which $\lambda$ and $\mu$ denote the Lamé Constants. Also, ($l_0$, $l_1$, $l_2$) represent independent material length scale parameters.

Using Eqs. (1) and (2a)-(2c) we have

$$\gamma_x = \frac{\partial^2 u}{\partial x^2} + \frac{1}{R}\frac{\partial w}{\partial x} + z\frac{\partial^2 \varphi_y}{\partial x^2} + y\left(\frac{1}{R}\frac{\partial \varphi_x}{\partial x} - \frac{\partial^2 \varphi_z}{\partial x^2}\right) + \frac{\partial v}{\partial x}\frac{\partial^2 v}{\partial x^2} + \frac{\partial w}{\partial x}\frac{\partial^2 w}{\partial x^2} \tag{18a}$$

$$\gamma_y = \frac{1}{R}\varphi_x - \frac{\partial \varphi_z}{\partial x} \tag{18b}$$

$$\gamma_z = \frac{\partial \varphi_y}{\partial x} \tag{18c}$$

$$\eta^{(1)}_{xxx} = \frac{2}{5}\left(\frac{\partial^2 u}{\partial x^2} + \frac{1}{R}\frac{\partial w}{\partial x} + z\frac{\partial^2 \varphi_y}{\partial x^2} + y\left(\frac{1}{R}\frac{\partial \varphi_x}{\partial x} - \frac{\partial^2 \varphi_z}{\partial x^2}\right) + \frac{\partial w}{\partial x}\frac{\partial^2 w}{\partial x^2} + \frac{1}{2R}\varphi_y\right) \tag{19a}$$

$$\eta^{(1)}_{yyy} = -\frac{1}{3}\left(\frac{\varphi_x}{R} - \frac{\partial \varphi_z}{\partial x} + \frac{\partial^2 v}{\partial x^2} - z\frac{\partial^2 \varphi_x}{\partial x^2} - \frac{\partial \varphi_z}{\partial x}\right) \tag{19b}$$

$$\eta^{(1)}_{zzz} = -\frac{1}{5}\left(\frac{\partial \varphi_y}{\partial x} + \frac{\partial^2 w}{\partial x^2} - \frac{1}{R}\frac{\partial u}{\partial x} + y\left(\frac{1}{R}\frac{\partial \varphi_z}{\partial x} - \frac{\partial^2 \varphi_x}{\partial x^2}\right) + \left(1 - \frac{z}{R}\right)\frac{\partial \varphi_y}{\partial x}\right) \tag{19c}$$

$$\eta^{(1)}_{xyz} = \eta^{(1)}_{yzx} = \eta^{(1)}_{zxy} = \eta^{(1)}_{xzy} = \eta^{(1)}_{zyx} = \eta^{(1)}_{yxz} = \frac{1}{6}\left(\frac{\varphi_z}{R} - 2\frac{\partial \varphi_x}{\partial x}\right) \tag{19d}$$

$$\eta^{(1)}_{xxy} = \eta^{(1)}_{xyx} = \eta^{(1)}_{yxx} = \frac{4}{5}\left(\frac{\varphi_x}{R} - \frac{\partial \varphi_z}{\partial x} + \frac{\partial^2 v}{\partial x^2} - z\frac{\partial^2 \varphi_x}{\partial x^2} - \frac{\partial \varphi_z}{\partial x}\right) \tag{19e}$$

$$\eta^{(1)}_{xxz} = \eta^{(1)}_{xzx} = \eta^{(1)}_{zxx} = \frac{4}{15}\left(\frac{\partial \varphi_y}{\partial x} + \frac{\partial^2 w}{\partial x^2} - \frac{1}{R}\frac{\partial u}{\partial x} + y\left(\frac{1}{R}\frac{\partial \varphi_z}{\partial x} - \frac{\partial^2 \varphi_x}{\partial x^2}\right) + \left(1 - \frac{z}{R}\right)\frac{\partial \varphi_y}{\partial x}\right) \tag{18f}$$

$$\eta^{(1)}_{yyx} = \eta^{(1)}_{yxy} = \eta^{(1)}_{xyy} = -\frac{1}{5}\left(\frac{\partial^2 u}{\partial x^2} + \frac{1}{R}\frac{\partial w}{\partial x} + z\frac{\partial^2 \varphi_y}{\partial x^2} + y\left(\frac{1}{R}\frac{\partial \varphi_x}{\partial x} - \frac{\partial^2 \varphi_z}{\partial x^2}\right) + \frac{\partial v}{\partial x}\frac{\partial^2 v}{\partial x^2} + \frac{\partial w}{\partial x}\frac{\partial^2 w}{\partial x^2}\right) + \frac{1}{15R}\varphi_y \tag{19g}$$

$$\eta^{(1)}_{yyz} = \eta^{(1)}_{yzy} = \eta^{(1)}_{zyy} = -\frac{1}{15}\left(\frac{\partial \varphi_y}{\partial x} + \frac{\partial^2 w}{\partial x^2} - \frac{1}{R}\frac{\partial u}{\partial x} + y\left(\frac{1}{R}\frac{\partial \varphi_z}{\partial x} - \frac{\partial^2 \varphi_x}{\partial x^2}\right) + \left(1 - \frac{z}{R}\right)\frac{\partial \varphi_y}{\partial x}\right) \tag{19h}$$

$$\eta^{(1)}_{zzx} = \eta^{(1)}_{zxz} = \eta^{(1)}_{xzz} = -\frac{1}{5}\left(\frac{\partial^2 u}{\partial x^2} + \frac{1}{R}\frac{\partial w}{\partial x} + z\frac{\partial^2 \varphi_y}{\partial x^2} + y\left(\frac{1}{R}\frac{\partial \varphi_x}{\partial x} - \frac{\partial^2 \varphi_z}{\partial x^2}\right) + \frac{\partial v}{\partial x}\frac{\partial^2 v}{\partial x^2} + \frac{\partial w}{\partial x}\frac{\partial^2 w}{\partial x^2}\right) - \frac{4}{15}\varphi_y \tag{19i}$$

$$\eta^{(1)}_{zzy} = \eta^{(1)}_{zyz} = \eta^{(1)}_{yzz} = -\frac{1}{15}\left(\frac{\varphi_x}{R} - \frac{\partial \varphi_z}{\partial x} + \frac{\partial^2 v}{\partial x^2} - z\frac{\partial^2 \varphi_x}{\partial x^2} - \frac{\partial \varphi_z}{\partial x}\right) \tag{19j}$$

$$\chi^s_{xx} = \frac{\partial \varphi_x}{\partial x} + \frac{1}{2R}\left(\frac{\partial v}{\partial x} - \frac{\partial \varphi_x}{\partial x} + \varphi_z\right) \tag{20a}$$

$$\chi^s_{yy} = -\frac{1}{2}\left(\frac{\partial \varphi_x}{\partial x} + \frac{\varphi_z}{R}\right) \tag{20b}$$

$$\chi^s_{zz} = -\frac{1}{2}\frac{\partial \varphi_x}{\partial x} \tag{20c}$$

$$\chi^s_{xy} = \frac{1}{4}\left(\frac{\partial \varphi_y}{\partial x} - \frac{\partial^2 w}{\partial x^2} - y\frac{\partial^2 \varphi_x}{\partial x^2} + \frac{1}{R}\frac{\partial u}{\partial x} + \frac{z}{R}\frac{\partial \varphi_y}{\partial x} - \frac{y}{R}\frac{\partial \varphi_z}{\partial x}\right) \tag{20d}$$

$$\chi^s_{xz} = \frac{1}{4}\left(\frac{\partial^2 v}{\partial x^2} - z\frac{\partial^2 \varphi_x}{\partial x^2} + \frac{\partial \varphi_z}{\partial x} - \frac{2}{R}\varphi_x\right) \tag{20e}$$

$$\chi^s_{yz} = \frac{1}{4R}\varphi_y \tag{20f}$$

Furthermore, the classical stresses tensor and the higher-order stresses terms can be simplified as

$$\sigma_{xx} = Q_{11}(z)\left(\frac{\partial u}{\partial x}+\frac{w}{R}+z\,\frac{\partial \varphi_y}{\partial x} +y\left(\frac{\varphi_x}{R}-\frac{\partial \varphi_z}{\partial x}\right)+\frac{1}{2}\left(\frac{\partial v}{\partial x}\right)^2 +\frac{1}{2}\left(\frac{\partial w}{\partial x}\right)^2-\alpha_{xx}\Delta T\right) \tag{21a}$$

$$\tau_{xy} = k_s Q_{22}(z)\left(\frac{\partial v}{\partial x}-z\,\frac{\partial \varphi_x}{\partial x}-\varphi_z\right) \tag{21b}$$

$$\tau_{xz} = k_s Q_{33}(z)\left(\left(\frac{\partial w}{\partial x}-\frac{u}{R}+\left(1-\frac{z}{R}\right)\varphi_y\right) +y\left(\frac{\varphi_z}{R}-\frac{\partial \varphi_x}{\partial x}\right)\right) \tag{21c}$$

$$p_x = 2\mu l_0^2\left(\frac{\partial^2 u}{\partial x^2}+\frac{1}{R}\frac{\partial w}{\partial x}+z\,\frac{\partial^2 \varphi_y}{\partial x^2} +y\left(\frac{1}{R}\frac{\partial \varphi_x}{\partial x}-\frac{\partial^2 \varphi_z}{\partial x^2}\right)+\frac{\partial v}{\partial x}\frac{\partial^2 v}{\partial x^2}+\frac{\partial w}{\partial x}\frac{\partial^2 w}{\partial x^2}\right) \tag{22a}$$

$$p_z = 2\mu l_0^2\,\frac{\partial \varphi_y}{\partial x} \tag{22b}$$

$$\tau_{xxx}^{(1)} = \frac{2}{5}\mu l_1^2\left(\frac{\partial^2 u}{\partial x^2}+\frac{1}{R}\frac{\partial w}{\partial x}+z\,\frac{\partial^2 \varphi_y}{\partial x^2} +y\left(\frac{1}{R}\frac{\partial \varphi_x}{\partial x}-\frac{\partial^2 \varphi_z}{\partial x^2}\right)+\frac{\partial v}{\partial x}\frac{\partial^2 v}{\partial x^2} +\frac{\partial w}{\partial x}\frac{\partial^2 w}{\partial x^2}+\frac{1}{2R}\varphi_y\right) \tag{23a}$$

$$\tau_{yyy}^{(1)} = -\frac{2}{3}\mu l_1^2\left(\frac{\varphi_x}{R}-\frac{\partial \varphi_z}{\partial x}+\frac{\partial^2 v}{\partial x^2}-z\,\frac{\partial^2 \varphi_x}{\partial x^2}-\frac{\partial \varphi_z}{\partial x}\right) \tag{23b}$$

$$\tau_{zzz}^{(1)} = -\frac{2}{5}\mu l_1^2\left(\frac{\partial \varphi_y}{\partial x}+\frac{\partial^2 w}{\partial x^2}-\frac{1}{R}\frac{\partial u}{\partial x} +y\left(\frac{1}{R}\frac{\partial \varphi_z}{\partial x}-\frac{\partial^2 \varphi_x}{\partial x^2}\right)+\left(1-\frac{z}{R}\right)\frac{\partial \varphi_y}{\partial x}\right) \tag{23c}$$

$$\tau_{xyz}^{(1)} = \frac{1}{3}\mu l_1^2\left(\frac{\varphi_z}{R}-2\frac{\partial \varphi_x}{\partial x}\right) \tag{23d}$$

$$\tau_{xxy}^{(1)} = \frac{8}{5}\mu l_1^2\left(\frac{\varphi_x}{R}-\frac{\partial \varphi_z}{\partial x}+\frac{\partial^2 v}{\partial x^2}-z\,\frac{\partial^2 \varphi_x}{\partial x^2}-\frac{\partial \varphi_z}{\partial x}\right) \tag{23e}$$

$$\tau_{xxz}^{(1)} = \frac{8}{15}\mu l_1^2\left(\frac{\partial \varphi_y}{\partial x}+\frac{\partial^2 w}{\partial x^2}-\frac{1}{R}\frac{\partial u}{\partial x} +y\left(\frac{1}{R}\frac{\partial \varphi_z}{\partial x}-\frac{\partial^2 \varphi_x}{\partial x^2}\right)+\left(1-\frac{z}{R}\right)\frac{\partial \varphi_y}{\partial x}\right) \tag{23f}$$

$$\tau_{yyx}^{(1)} = -\frac{2}{5}\mu l_1^2\left(\frac{\partial^2 u}{\partial x^2}+\frac{1}{R}\frac{\partial w}{\partial x}+z\,\frac{\partial^2 \varphi_y}{\partial x^2} +y\left(\frac{1}{R}\frac{\partial \varphi_x}{\partial x}-\frac{\partial^2 \varphi_z}{\partial x^2}\right)+\frac{\partial v}{\partial x}\frac{\partial^2 v}{\partial x^2}+\frac{\partial w}{\partial x}\frac{\partial^2 w}{\partial x^2}\right) +\frac{2}{15R}\mu l_1^2\varphi_y \tag{23g}$$

$$\tau_{yyz}^{(1)} = -\frac{2}{15}\mu l_1^2\left(\frac{\partial \varphi_y}{\partial x}+\frac{\partial^2 w}{\partial x^2}-\frac{1}{R}\frac{\partial u}{\partial x} +y\left(\frac{1}{R}\frac{\partial \varphi_z}{\partial x}-\frac{\partial^2 \varphi_x}{\partial x^2}\right)+\left(1-\frac{z}{R}\right)\frac{\partial \varphi_y}{\partial x}\right) \tag{23h}$$

$$\tau_{zzx}^{(1)} = -\frac{2}{5}\mu l_1^2\left(\frac{\partial^2 u}{\partial x^2}+\frac{1}{R}\frac{\partial w}{\partial x}+z\,\frac{\partial^2 \varphi_y}{\partial x^2} +y\left(\frac{1}{R}\frac{\partial \varphi_x}{\partial x}-\frac{\partial^2 \varphi_z}{\partial x^2}\right)+\frac{\partial v}{\partial x}\frac{\partial^2 v}{\partial x^2}+\frac{\partial w}{\partial x}\frac{\partial^2 w}{\partial x^2}\right) -\frac{8}{15}\mu l_1^2\varphi_y \tag{23i}$$

$$\tau_{zzy}^{(1)} = -\frac{2}{15}\mu l_1^2\left(\frac{\varphi_x}{R}-\frac{\partial \varphi_z}{\partial x}+\frac{\partial^2 v}{\partial x^2}-z\,\frac{\partial^2 \varphi_x}{\partial x^2}-\frac{\partial \varphi_z}{\partial x}\right) \tag{23j}$$

$$\tau_{zzx}^{(1)} = -\frac{2}{5}\mu l_1^2\left(\frac{\partial^2 u}{\partial x^2}+\frac{1}{R}\frac{\partial w}{\partial x}+z\,\frac{\partial^2 \varphi_y}{\partial x^2} +y\left(\frac{1}{R}\frac{\partial \varphi_x}{\partial x}-\frac{\partial^2 \varphi_z}{\partial x^2}\right)+\frac{\partial v}{\partial x}\frac{\partial^2 v}{\partial x^2}+\frac{\partial w}{\partial x}\frac{\partial^2 w}{\partial x^2}\right) -\frac{8}{15}\mu l_1^2\varphi_y \tag{23k}$$

$$\tau_{zzy}^{(1)} = -\frac{2}{15}\mu l_1^2\left(\frac{\varphi_x}{R}-\frac{\partial \varphi_z}{\partial x}+\frac{\partial^2 v}{\partial x^2}-z\,\frac{\partial^2 \varphi_x}{\partial x^2}-\frac{\partial \varphi_z}{\partial x}\right) \tag{23l}$$

$$m_{xx}^s = 2\mu l_2^2\left(\frac{\partial \varphi_x}{\partial x}+\frac{1}{2R}\left(\frac{\partial v}{\partial x}-z\,\frac{\partial \varphi_x}{\partial x}+\varphi_z\right)\right) \tag{24a}$$

$$m_{yy}^s = -\mu l_2^2\left(\frac{\partial \varphi_x}{\partial x}+\frac{\varphi_z}{R}\right) \tag{24b}$$

$$m_{zz}^s = -\mu l_2^2\,\frac{\partial \varphi_x}{\partial x} \tag{24c}$$

$$m_{xy}^{s}=\frac{\mu l_2^2}{2}\left(\begin{array}{l}\dfrac{\partial\varphi_y}{\partial x}-\dfrac{\partial^2 w}{\partial x^2}-y\dfrac{\partial^2\varphi_x}{\partial x^2}\\ +\dfrac{1}{R}\dfrac{\partial u}{\partial x}+\dfrac{z}{R}\dfrac{\partial\varphi_y}{\partial x}-\dfrac{y}{R}\dfrac{\partial\varphi_z}{\partial x}\end{array}\right) \tag{24d}$$

$$m_{xz}^{s}=\frac{\mu l_2^2}{2}\left(\frac{\partial^2 v}{\partial x^2}-z\frac{\partial^2\varphi_x}{\partial x^2}+\frac{\partial\varphi_z}{\partial x}-\frac{2}{R}\varphi_x\right) \tag{24e}$$

$$m_{yz}^{s}=\frac{\mu l_2^2}{2R}\varphi_y \tag{24f}$$

in which $\alpha_{xx}$ and $\Delta T$ are thermal expansion and temperature difference, respectively and

$$Q_{11}(z)=\frac{E(z)}{1-\nu_{12}\nu_{21}}, \tag{24g}$$

$$Q_{22}(z)=Q_{33}(z)=G_{12}(z) \tag{24h}$$

Eventually, the total potential energy of the structure can be expressed as

$$\begin{aligned}U_m=&\frac{1}{2}\int_{\Omega}\left(\sigma_{xx}\varepsilon_{xx}+2\tau_{xy}\varepsilon_{xy}+2\tau_{xz}\varepsilon_{xz}\right.\\&+p_x\gamma_x+p_y\gamma_y+p_z\gamma_z+\tau_{xxx}^{(1)}\eta_{xxx}^{(1)}+\tau_{yyy}^{(1)}\eta_{yyy}^{(1)}\\&+\tau_{zzz}^{(1)}\eta_{zzz}^{(1)}+6\tau_{xyz}^{(1)}\eta_{xyz}^{(1)}+3\tau_{xxy}^{(1)}\eta_{xxy}^{(1)}+3\tau_{xxz}^{(1)}\eta_{xxz}^{(1)}\\&+3\tau_{yyx}^{(1)}\eta_{yyx}^{(1)}+3\tau_{yyz}^{(1)}\eta_{yyz}^{(1)}+3\tau_{zzx}^{(1)}\eta_{zzx}^{(1)}+3\tau_{zzy}^{(1)}\eta_{zzy}^{(1)}\\&+m_{xx}^{s}\chi_{xx}^{s}+m_{yy}^{s}\chi_{yy}^{s}+m_{zz}^{s}\chi_{zz}^{s}+2m_{xy}^{s}\chi_{xy}^{s}\\&\left.+2m_{xz}^{s}\chi_{xz}^{s}+2m_{yz}^{s}\chi_{yz}^{s}\right)dV\end{aligned} \tag{25}$$

The kinetic energy of the curved microbeam can be written as

$$K=\frac{1}{2}\int_0^L\int_A\rho\left(\left(\frac{\partial u_x}{\partial t}\right)^2+\left(\frac{\partial u_y}{\partial t}\right)^2+\left(\frac{\partial u_z}{\partial t}\right)^2\right)dA\,dx, \tag{26}$$

in which $\rho$ denotes the mass density of the nanocomposite structure. Also, the work done by the external forces is subjected by surrounding viscoelastic foundation and axial magnetic field which can be calculated as below (Shen and Zhang 2011, Kolahchi *et al*. 2015)

$$W=\frac{1}{2}\int_0^L\left(\begin{array}{l}-k_w w-k_{2w}w^3-c_d\dfrac{\partial w}{\partial t}\\+G_\xi(\cos^2\alpha)\dfrac{\partial^2 w}{\partial x^2}+G_\zeta(\sin^2\alpha)\dfrac{\partial^2 w}{\partial x^2}\\+\eta A H_x^2\dfrac{\partial^2 w}{\partial x^2}+F_0\cos(\Omega t)\delta(x-x_0)\end{array}\right)w\,dx, \tag{27}$$

where $k_w$ and $k_{2w}$ indicate the linear and nonlinear spring constant of the Winkler type, respectively. Also, $c_d$, $G_\xi$ and $G_\zeta$ represent the damper constant of foundation and the shear constants in $\xi$ and $\zeta$ directions, respectively. Moreover, $\eta$ is the magnetic field permeability and $H_x$ denotes the axial magnetic field; $F_0$ and $\Omega$ represent amplitude and excitation frequency of the concentrated transverse harmonic external force, respectively. $\delta$ and $x_0$ denote Dirac delta function and location of harmonic load. The foundation stiffness $k_w$ for soft medium can be considered as below

$$K_w=\frac{E_0}{4L(1-\nu_0^2)(2-c_1)^2}\left[5-\left(2\gamma_1^2+6\gamma_1+5\right)\exp(-2\gamma_1)\right], \tag{28a}$$

in which

$$c_1=(\gamma_1+2)\exp(-\gamma_1), \tag{28b}$$

$$\gamma_1=\frac{H_s}{L}, \tag{28c}$$

$$E_0=\frac{E_s}{(1-\nu_s^2)}, \tag{28d}$$

$$\nu_0=\frac{\nu_s}{(1-\nu_s)}, \tag{28e}$$

where $E_s$, $\nu_s$, $H_s$ denote Young's modulus, Poisson's ratio and depth of the foundation, respectively. Here, $E_s$ is considered to be temperature-dependent despite $\nu_s$ is assumed to be a constant.

Substituting Eqs. (25)-(27) into Eq. (13), the motion equations can be derived as follows

$$\begin{aligned}&\frac{\partial N_x}{\partial x}+\frac{Q_{xz}}{R}-\frac{2}{5}\frac{\partial^2 T_{xxx}}{\partial x^2}+\frac{1}{5R}\frac{\partial T_{zzz}}{\partial x}\\&-\frac{4}{5R}\frac{\partial T_{xxz}}{\partial x}+\frac{3}{5}\frac{\partial^2 T_{yyx}}{\partial x^2}+\frac{1}{5R}\frac{\partial T_{yyz}}{\partial x}\\&+\frac{3}{5}\frac{\partial^2 T_{zzx}}{\partial x^2}-\frac{\partial^2 P_x}{\partial x^2}+\frac{1}{2R}\frac{\partial Y_{xy}}{\partial x}\\&=I_1\frac{\partial^2 u}{\partial t^2}-I_2\frac{\partial^2\varphi_y}{\partial t^2}+I_3\frac{\partial^2\varphi_z}{\partial t^2}\end{aligned} \tag{29}$$

$$\begin{aligned}&\frac{\partial Q_{xy}}{\partial x}+\frac{\partial}{\partial x}\left(N_x\frac{\partial v}{\partial x}\right)+\frac{2}{5}\frac{\partial}{\partial x}\left(T_{xxx}\frac{\partial^2 v}{\partial x^2}\right)\\&-\frac{2}{5}\frac{\partial^2}{\partial x^2}\left(T_{xxx}\frac{\partial v}{\partial x}\right)+\frac{1}{3}\frac{\partial^2 T_{yyy}}{\partial x^2}-\frac{4}{5}\frac{\partial^2 T_{xxy}}{\partial x^2}\\&-\frac{3}{5}\frac{\partial}{\partial x}\left(T_{yyx}\frac{\partial^2 v}{\partial x^2}\right)+\frac{3}{5}\frac{\partial^2}{\partial x^2}\left(T_{yyx}\frac{\partial v}{\partial x}\right)\\&+\frac{1}{5}\frac{\partial^2 T_{zzy}}{\partial x^2}-\frac{3}{5}\frac{\partial}{\partial x}\left(T_{zzx}\frac{\partial^2 v}{\partial x^2}\right)+\frac{3}{5}\frac{\partial^2}{\partial x^2}\left(T_{zzx}\frac{\partial v}{\partial x}\right)\\&+\frac{\partial}{\partial x}\left(P_x\frac{\partial^2 v}{\partial x^2}\right)-\frac{\partial^2}{\partial x^2}\left(P_x\frac{\partial v}{\partial x}\right)+\frac{1}{2R}\frac{\partial Y_x}{\partial x}\\&-\frac{1}{2}\frac{\partial^2 Y_{xz}}{\partial x^2}=I_1\frac{\partial^2 v}{\partial t^2}+I_2\frac{\partial^2\varphi_x}{\partial t^2}\end{aligned} \tag{30}$$

$$
\begin{aligned}
&-\frac{N_x}{R}+\frac{\partial Q_{xz}}{\partial x}+\frac{2}{5R}\frac{\partial T_{xxx}}{\partial x}+\frac{2}{5}\frac{\partial}{\partial x}\left(T_{xxx}\frac{\partial^2 w}{\partial x^2}\right)\\
&-\frac{2}{5}\frac{\partial^2}{\partial x^2}\left(T_{xxx}\frac{\partial w}{\partial x}\right)-\frac{4}{5}\frac{\partial^2 T_{xxz}}{\partial x^2}\\
&-\frac{3}{5R}\frac{\partial T_{yyx}}{\partial x}-\frac{3}{5}\frac{\partial}{\partial x}\left(T_{yyx}\frac{\partial^2 w}{\partial x^2}\right)+\frac{3}{5}\frac{\partial^2}{\partial x^2}\left(T_{yyx}\frac{\partial w}{\partial x}\right)\\
&+\frac{1}{5}\frac{\partial^2 T_{yyz}}{\partial x^2}-\frac{3}{5R}\frac{\partial T_{zzx}}{\partial x}-\frac{3}{5}\frac{\partial}{\partial x}\left(T_{zzx}\frac{\partial^2 w}{\partial x^2}\right)\\
&+\frac{3}{5}\frac{\partial^2}{\partial x^2}\left(T_{zzx}\frac{\partial w}{\partial x}\right)+\frac{1}{R}\frac{\partial P_x}{\partial x}+\frac{\partial}{\partial x}\left(P_x\frac{\partial^2 w}{\partial x^2}\right)\\
&-\frac{\partial^2}{\partial x^2}\left(P_x\frac{\partial w}{\partial x}\right)+\frac{1}{2}\frac{\partial^2 Y_{xy}}{\partial x^2}+N_x^T\frac{\partial^2 w}{\partial x^2}-k_w w\\
&-k_{2w}w^3-c_d\frac{\partial w}{\partial t}+G_\xi\left(\cos^2(\alpha)\right)\frac{\partial^2 w}{\partial x^2}+G_\zeta\left(\sin^2(\alpha)\right)\frac{\partial^2 w}{\partial x^2}\\
&+\eta A H_x^2\frac{\partial^2 w}{\partial x^2}+F_0\cos(\Omega t)\delta(x-x_0)=I_1\frac{\partial^2 w}{\partial t^2}-I_3\frac{\partial^2 \varphi_x}{\partial t^2}
\end{aligned}
\tag{31}
$$

$$
\begin{aligned}
&-\frac{1}{R}M_x^2-\frac{\partial P_{xy}}{\partial x}-\frac{\partial^2 P_{xz}}{\partial x^2}+\frac{2}{5R}\frac{\partial M_{xxx}^2}{\partial x}\\
&+\frac{1}{3R}T_{yyy}-\frac{1}{3}\frac{\partial^2 M_{yyy}}{\partial x^2}-\frac{1}{5}\frac{\partial^2 M_{zzz}^2}{\partial x^2}\\
&-2\frac{\partial T_{xyz}}{\partial x}-\frac{12}{5R}T_{xxy}+\frac{12}{5}\frac{\partial^2 M_{xxy}^1}{\partial x^2}\\
&+\frac{4}{5}\frac{\partial^2 M_{xxz}^2}{\partial x^2}-\frac{3}{5R}\frac{\partial M_{yyx}^2}{\partial x}-\frac{1}{5}\frac{\partial^2 M_{yyz}^2}{\partial x^2}\\
&-\frac{3}{5R}\frac{\partial M_{zzx}^2}{\partial x}+\frac{1}{5R}T_{zzy}-\frac{2}{5}\frac{\partial^2 M_{zzy}}{\partial x^2}\\
&+\frac{1}{R}\frac{\partial S_x^2}{\partial x}-\frac{1}{R}P_y+\frac{\partial Y_x}{\partial x}-\frac{1}{2R}\frac{\partial X_x}{\partial x}\\
&-\frac{1}{2}\frac{\partial Y_y}{\partial x}-\frac{1}{2}\frac{\partial Y_z}{\partial x}+\frac{1}{2}\frac{\partial^2 X_{xy}^2}{\partial x^2}+\frac{1}{2}\frac{\partial^2 X_{xz}}{\partial x^2}\\
&=\left(I_5+I_6\right)\frac{\partial^2 \varphi_x}{\partial t^2}+I_2\frac{\partial^2 v}{\partial t^2}-I_3\frac{\partial^2 w}{\partial t^2}
\end{aligned}
\tag{32}
$$

$$
\begin{aligned}
&\frac{\partial M_x^1}{\partial x}-Q_{xz}+\frac{1}{R}P_{xz}^1-\frac{2}{5}\frac{\partial^2 M_{xxx}^1}{\partial x^2}-\frac{1}{5R}T_{xxx}\\
&-\frac{2}{5}\frac{\partial T_{zzz}}{\partial x}+\frac{1}{5R}\frac{\partial M_{zzz}^1}{\partial x}+\frac{8}{5}\frac{\partial T_{xxz}}{\partial x}-\frac{4}{5R}\frac{\partial M_{xxz}^1}{\partial x}\\
&+\frac{3}{5}\frac{\partial^2 M_{yyx}^1}{\partial x^2}-\frac{1}{5R}T_{yyx}-\frac{2}{5}\frac{\partial T_{yyz}}{\partial x}+\frac{1}{5R}\frac{\partial M_{yyz}^1}{\partial x}\\
&+\frac{4}{5R}T_{zzx}+\frac{3}{5}\frac{\partial^2 M_{zzx}^1}{\partial x^2}-\frac{\partial^2 S_x^1}{\partial x^2}+\frac{\partial P_z}{\partial x}\\
&+\frac{1}{2}\frac{\partial Y_{xy}}{\partial x}+\frac{1}{2R}\frac{\partial X_{xy}^1}{\partial x}-\frac{1}{2R}Y_{yz}\\
&=I_5\frac{\partial^2 \varphi_y}{\partial t^2}-I_2\frac{\partial^2 u}{\partial t^2}+I_4\frac{\partial^2 \varphi_z}{\partial t^2}
\end{aligned}
\tag{33}
$$

$$
\begin{aligned}
&-\frac{\partial M_x^2}{\partial x}+Q_{xy}-\frac{P_{xz}^2}{R}+\frac{2}{5}\frac{\partial^2 M_{xxx}^2}{\partial x^2}+\frac{2}{3}\frac{\partial T_{yyy}}{\partial x}\\
&-\frac{1}{5R}\frac{\partial^2 M_{zzz}^2}{\partial x^2}-\frac{1}{R}T_{xyz}-\frac{12}{5}\frac{\partial T_{xxy}}{\partial x}+\frac{4}{5R}\frac{\partial M_{xxz}^2}{\partial x}\\
&-\frac{3}{5}\frac{\partial^2 M_{yyx}^2}{\partial x^2}-\frac{1}{5R}\frac{\partial M_{yyz}^2}{\partial x}-\frac{3}{5}\frac{\partial^2 M_{zzx}^2}{\partial x^2}+\frac{2}{5}\frac{\partial T_{zzy}}{\partial x}\\
&+\frac{\partial^2 S_x^2}{\partial x^2}-\frac{\partial P_y}{\partial x}-\frac{Y_x}{2R}+\frac{Y_y}{2R}-\frac{1}{2R}\frac{\partial X_{xy}^2}{\partial x}\\
&+\frac{1}{2}\frac{\partial Y_{xz}}{\partial x}=I_6\frac{\partial^2 \varphi_z}{\partial t^2}+I_3\frac{\partial^2 u}{\partial t^2}+I_4\frac{\partial^2 \varphi_y}{\partial t^2}
\end{aligned}
\tag{34}
$$

where the moment of inertias and the thermal force can be defined as

$$
\left(I_1,I_2,I_3,I_4,I_5,I_6\right)=\int_{-h/2}^{h/2}\int_{-b/2}^{b/2}\rho(z)\left(1,z,y,zy,z^2,y^2\right)dydz, \tag{35a}
$$

$$
N_x^T=-\int_s\left(Q_{11}(z)\alpha_{xx}\Delta T\right)dA. \tag{35b}
$$

The stress resultants which mentioned in above equations are defined in Appendix A.

Moreover, the size-dependent various boundary conditions at both ends of the composite curved microbeam can be expressed based on Hamilton's principle as follows

- **Simply Supported-Simply Supported (SS)**

At $x = 0, L$

$$
w=v=\varphi_x=\frac{\partial u}{\partial x}=\frac{\partial \varphi_y}{\partial x}=\frac{\partial \varphi_z}{\partial x}=0, \tag{36a}
$$

$$
\begin{aligned}
&-N_x+\frac{2}{5}\frac{\partial T_{xxx}}{\partial x}-\frac{1}{5R}T_{zzz}+\frac{4}{5R}T_{xxz}\\
&-\frac{3}{5}\frac{\partial T_{yyx}}{\partial x}-\frac{1}{5R}T_{yyz}-\frac{3}{5}\frac{\partial T_{zzx}}{\partial x}\\
&+\frac{\partial P_x}{\partial x}-\frac{1}{2R}Y_{xy}=0,
\end{aligned}
\tag{36b}
$$

$$
\begin{aligned}
&-M_x^1+\frac{2}{5}\frac{\partial M_{xxx}^1}{\partial x}+\frac{2}{5}T_{zzz}-\frac{1}{5R}M_{zzz}^1-\frac{8}{5}T_{xxz}\\
&+\frac{4}{5R}M_{xxz}^1-\frac{3}{5}\frac{\partial M_{yyx}^1}{\partial x}+\frac{2}{5}T_{yyz}-\frac{1}{5R}M_{yyz}^1\\
&-\frac{3}{5}\frac{\partial M_{zzx}^1}{\partial x}+\frac{\partial S_x^1}{\partial x}-P_z-\frac{1}{2}Y_{xy}-\frac{1}{2R}X_{xy}^1=0,
\end{aligned}
\tag{36c}
$$

$$
\begin{aligned}
&M_x^2-\frac{2}{5}\frac{\partial M_{xxx}^2}{\partial x}-\frac{2}{3}T_{yyy}+\frac{1}{5R}\frac{\partial M_{zzz}^2}{\partial x}+\frac{4}{5}T_{xxy}\\
&-\frac{4}{5R}M_{xxz}^2+\frac{3}{5}\frac{\partial M_{yyx}^2}{\partial x}+\frac{1}{5R}M_{yyz}^2+\frac{3}{5}\frac{\partial M_{zzx}^2}{\partial x}\\
&-\frac{2}{5}T_{zzy}-\frac{\partial S_x^2}{\partial x}+P_y+\frac{1}{2R}X_{xy}^2-\frac{1}{2}Y_{xz}=0,
\end{aligned}
\tag{36d}
$$

$$\frac{2}{5}T_{xxx}\frac{\partial w}{\partial x}-\frac{1}{5}T_{zzz}+\frac{4}{5}T_{xxz}-\frac{3}{5}T_{yyx}\frac{\partial w}{\partial x}-\frac{1}{5}T_{yyz}-\frac{3}{5}T_{zzx}\frac{\partial w}{\partial x}+P_x\frac{\partial w}{\partial x}-\frac{1}{2}Y_{xy}=0, \tag{36e}$$

$$\frac{2}{5}T_{xxx}\frac{\partial v}{\partial x}-\frac{1}{5}T_{yyy}-\frac{3}{5}T_{yyx}\frac{\partial v}{\partial x}+\frac{4}{5}T_{xxy}-\frac{1}{5}T_{zzy}-\frac{3}{5}T_{zzx}\frac{\partial v}{\partial x}+P_x\frac{\partial v}{\partial x}+\frac{1}{2}Y_{xz}=0, \tag{36f}$$

$$P_{xz}+\frac{1}{3}M_{yyy}+\frac{1}{5}M^{2}_{zzz}-\frac{4}{5}M_{xxy}-\frac{4}{5}M^{2}_{xxz}+\frac{1}{5}M^{2}_{yyz}+\frac{2}{5}M_{zzy}-\frac{1}{2}X^{2}_{xy}-\frac{1}{2}X_{xz}=0. \tag{36g}$$

➢ **Clamped-Clamped (CC)**

At $x = 0, L$

$$u=w=v=\varphi_x=\varphi_y=\varphi_z=\frac{\partial u}{\partial x}=\frac{\partial v}{\partial x}=\frac{\partial w}{\partial x}=\frac{\partial \varphi_x}{\partial x}=\frac{\partial \varphi_y}{\partial x}=\frac{\partial \varphi_z}{\partial x}=0. \tag{37}$$

➢ **Clamped-Simply Supported (CS)**

At $x = 0$

$$u=w=v=\varphi_x=\varphi_y=\varphi_z=\frac{\partial u}{\partial x}=\frac{\partial v}{\partial x}=\frac{\partial w}{\partial x}=\frac{\partial \varphi_x}{\partial x}=\frac{\partial \varphi_y}{\partial x}=\frac{\partial \varphi_z}{\partial x}=0. \tag{38a}$$

At $x = L$

$$w=v=\varphi_x=\frac{\partial u}{\partial x}=\frac{\partial \varphi_y}{\partial x}=\frac{\partial \varphi_z}{\partial x}=0. \tag{38b}$$

$$-N_x+\frac{2}{5}\frac{\partial T_{xxx}}{\partial x}-\frac{1}{5R}T_{zzz}+\frac{4}{5R}T_{xxz}-\frac{3}{5}\frac{\partial T_{yyx}}{\partial x}-\frac{1}{5R}T_{yyz}-\frac{3}{5}\frac{\partial T_{zzx}}{\partial x}+\frac{\partial P_x}{\partial x}-\frac{1}{2R}Y_{xy}=0, \tag{38c}$$

$$-M^{1}_{x}+\frac{2}{5}\frac{\partial M^{1}_{xxx}}{\partial x}+\frac{2}{5}T_{zzz}-\frac{1}{5R}M^{1}_{zzz}-\frac{8}{5}T_{xxz}+\frac{4}{5R}M^{1}_{xxz}-\frac{3}{5}\frac{\partial M^{1}_{yyx}}{\partial x}+\frac{2}{5}T_{yyz}-\frac{1}{5R}M^{1}_{yyz}-\frac{3}{5}\frac{\partial M^{1}_{zzx}}{\partial x}+\frac{\partial S^{1}_{x}}{\partial x}-P_z-\frac{1}{2}Y_{xy}-\frac{1}{2R}X^{1}_{xy}=0, \tag{38d}$$

$$M^{2}_{x}-\frac{2}{5}\frac{\partial M^{2}_{xxx}}{\partial x}-\frac{2}{3}T_{yyy}+\frac{1}{5R}\frac{\partial M^{2}_{zzz}}{\partial x}+\frac{4}{5}T_{xxy}-\frac{4}{5R}M^{2}_{xxz}+\frac{3}{5}\frac{\partial M^{2}_{yyx}}{\partial x}+\frac{1}{5R}M^{2}_{yyz}+\frac{3}{5}\frac{\partial M^{2}_{zzx}}{\partial x}-\frac{2}{5}T_{zzy}-\frac{\partial S^{2}_{x}}{\partial x}+P_y+\frac{1}{2R}X^{2}_{xy}-\frac{1}{2}Y_{xz}=0, \tag{38e}$$

$$\frac{2}{5}T_{xxx}\frac{\partial w}{\partial x}-\frac{1}{5}T_{zzz}+\frac{4}{5}T_{xxz}-\frac{3}{5}T_{yyx}\frac{\partial w}{\partial x}-\frac{1}{5}T_{yyz}-\frac{3}{5}T_{zzx}\frac{\partial w}{\partial x}+P_x\frac{\partial w}{\partial x}-\frac{1}{2}Y_{xy}=0, \tag{38f}$$

$$\frac{2}{5}T_{xxx}\frac{\partial v}{\partial x}-\frac{1}{5}T_{yyy}-\frac{3}{5}T_{yyx}\frac{\partial v}{\partial x}+\frac{4}{5}T_{xxy}-\frac{1}{5}T_{zzy}-\frac{3}{5}T_{zzx}\frac{\partial v}{\partial x}+P_x\frac{\partial v}{\partial x}+\frac{1}{2}Y_{xz}=0, \tag{38g}$$

$$P_{xz}+\frac{1}{3}M_{yyy}+\frac{1}{5}M^{2}_{zzz}-\frac{4}{5}M_{xxy}-\frac{4}{5}M^{2}_{xxz}+\frac{1}{5}M^{2}_{yyz}+\frac{2}{5}M_{zzy}-\frac{1}{2}X^{2}_{xy}-\frac{1}{2}X_{xz}=0. \tag{38h}$$

## 4. Solving the problem

### *4.1 DQ method*

In this part, DQ method is applied to solve the governing equations of the curved nanocomposite beam. For this goal, the governing differential equations are turned into a set of first order algebraic equations employing the weighting coefficients. DQ method approximates a derivative of a function at a given discrete point as a weighted linear sum of the function values at all discrete points selected in the solution domain. Therefore, the one-dimensional derivative of the function may be expressed as below (Kolahchi and Moniribidgoli 2016, Kolahchi *et al*. 2015, 2016a, b, 2017a, b)

$$\frac{d^n f(x_i)}{dx^n}=\sum_{j=1}^{N}C_{ij}^{(n)}f(x_j) \qquad n=1,...,N-1. \tag{39}$$

where $f(x)$ denotes the mentioned function, $N$ represents the number of the grid points, $x_i$ denotes a sample point of the function domain, $f_i$ is the value of the function at $i$th sample point and $C_{ij}$ represent the weighting coefficients. So, it can be concluded that choosing the grid points and weighting coefficients are significant factors for obtaining the accurate results. The grid points are defined based on the Chebyshev polynomials which are considered as below

$$x_i=\frac{L}{2}\left[1-\cos\left(\frac{i-1}{N-1}\right)\pi\right] \quad i=1,...,N \tag{40}$$

On the basis of Chebyshev polynomials, the grid points

are closer together near the borders and in distant parts of the borders, they are considered away from each other.

Also, the weighting coefficients can be considered as the following simple algebraic relations

$$A_{ij}^{(1)}=\begin{cases}\dfrac{M(x_i)}{M(x_j)(x_i-x_j)} & \text{for} \quad i\neq j,\quad i,j=1,2,...,N,\\ -\sum\limits_{\substack{j=1\\ i\neq j}}^{N}A_{ij}^{(1)} & \text{for} \quad i=j,\quad i,j=1,2,...,N\end{cases} \tag{41}$$

where

$$M(x_i)=\prod_{\substack{j=1\\ j\neq i}}^{N}(x_i-x_j) \tag{42}$$

Moreover, the higher-order derivatives are defined as below

$$A_{ij}^{(n)}=n\left(A_{ii}^{(n-1)}A_{ij}^{(1)}-\pi ctg\left(\frac{x_i-x_j}{2}\right)\pi\right) \tag{43}$$

### 4.2 IQ method

IQ method is also on the basis of the analysis of a high-order polynomial approximation in a linear vector space. As a general case, the integral of $f(x)$ over a part of the whole domain can be approximated using a linear combination of all the functional values in the whole domain as the following form (Shu *et al*. 1995)

$$\int_{x_i}^{x_j}f(x)dx=\sum_{k=1}^{N}C_k^{ij}f(x_k),\qquad with\ C_k^{ij}=w_{jk}^{I}-w_{ik}^{I}, \tag{44}$$

in which $x_i$ and $x_j$ represents the numbers which can be altered; $w^I = a^{-1}$ that we have

$$a_{ij}=\frac{x_i-c}{x_j-c}A_{ij}^{(1)}\quad when\ i\neq j \tag{45}$$

$$a_{ii}=A_{ii}^{(1)}+\frac{1}{x_i-c}\quad when\ i\neq j \tag{46}$$

where $A_{ij}^{(1)}$ denotes the weighting coefficient of the first-order derivative in DQ method. Also, $c$ indicates a constant which are considered as 0.01 (Shu *et al*. 1995). Finally, employing DQ-IQ methods, the motion equations can be rewritten in a compact matrix form as below

$$[K_L+K_{NL}]\begin{bmatrix}d_b(t)\\ d_d(t)\end{bmatrix}+[C]\begin{bmatrix}\dot{d}_b(t)\\ \dot{d}_d(t)\end{bmatrix}+[M]\begin{bmatrix}\ddot{d}_b(t)\\ \ddot{d}_d(t)\end{bmatrix}=\begin{bmatrix}[0]\\ Q(t)\end{bmatrix}, \tag{47}$$

in which $[d]=[u\ v\ w\ \varphi_x\ \varphi_y\ \varphi_z]^T$; the indexes of $b$ and $d$ are related to boundary and domain points, respectively. Furthermore, $[K_L]$, $[K_{NL}]$ and $[C]$ represent the linear and nonlinear stiffness matrices and damping matrix, respectively. Also, $[M]$ denotes the mass matrix.

### 4.3 Newmark time integration scheme

In this section, the average acceleration method of Newmark-$\beta$ (Simsek and Kocaturk 2009) in conjunction with an iteration method is employed. This method reduces the time domain Eq. (47) as the following set of nonlinear algebraic equations

$$K^*(d_{i+1})=Q_{i+1}, \tag{48}$$

in which subscript $i + 1$ indicates the number of steps for the concerned time $t = t_{i+1}$. Also, $K^*(d_{i+1})$ represents the effective stiffness matrix and $Q_{i+1}$ denotes the effective load vector, which may be defined as below

$$K^*(d_{i+1})=K_L+K_{NL}(d_{i+1})+\alpha_0M+\alpha_1C, \tag{49}$$

$$\begin{aligned}Q_{i+1}^{*}&=Q_{i+1}+M\left(\alpha_0d_i+\alpha_2\dot{d}_i+\alpha_3\ddot{d}_i\right)\\ &+C\left(\alpha_1d_i+\alpha_4\dot{d}_i+\alpha_5\ddot{d}_i\right),\end{aligned} \tag{50}$$

where

$$\begin{aligned}&\alpha_0=\frac{1}{\chi\Delta t^2},\quad \alpha_1=\frac{\gamma}{\chi\Delta t},\quad \alpha_2=\frac{1}{\chi\Delta t},\\ &\alpha_3=\frac{1}{2\chi}-1,\quad \alpha_4=\frac{\gamma}{\chi}-1,\alpha_5=\frac{\Delta t}{2}\left(\frac{\gamma}{\chi}-2\right),\\ &\alpha_6=\Delta t\left(1-\gamma\right),\qquad \alpha_7=\Delta t\gamma,\end{aligned} \tag{51}$$

in which $\gamma = 0.5$ and $\chi = 0.25$ (Simsek and Kocaturk 2009). According to the mentioned iteration method, Eq. (48) can be solved for any fixed time and then, the new acceleration and velocity vectors can be achieved as below

$$\ddot{d}_{i+1}=\alpha_0(d_{i+1}-d_i)-\alpha_2\dot{d}_i-\alpha_3\ddot{d}_i, \tag{52}$$

$$\dot{d}_{i+1}=\dot{d}_i+\alpha_6\ddot{d}_i+\alpha_7\ddot{d}_{i+1}, \tag{53}$$

Similarly, the mentioned procedure can be repeated for each time step.

## 5. Results and discussion

To investigate the in-plane and out-of-plane forced vibration of FG-CNTs reinforced curved microbeam, a curved microbeam with matrix material made of Poly methyl methacrylate (PMMA) is chosen with Poisson's ratios of $\nu_m$ = 0.34, temperature-dependent thermal coefficient of $\alpha_m = (1+0.0005\Delta T)\times10^{-6}/K$ and temperature-dependent Young moduli of $E_m = (3.52 - 0.0034T)$ GPa in which $T = T_0 + \Delta T$ and $T_0$ = 300 K (room temperature). The structure is reinforced by (10, 10) SWCNTs with the mechanical properties listed in Table 1. Moreover, the temperature-dependent elastic foundation is composed of Poly dimethylsiloxane (PDMS) with Poisson's ratios of $\nu_s$ = 0.48 and Young moduli of $E_s = (3.22 - 0.0034T)$ GPa (Shen and Zhang 2011).

Table 1 Temperature-dependent material properties of (10, 10) SWCNT ($L$ = 9.26 nm, $R$ = 0.68 nm, $h$ = 0.067 nm, $\upsilon_{12}^{CNT} = 0.175$)

| Temperature (K) | $E_{11}^{CNT}$ (TPa) | $E_{22}^{CNT}$ (TPa) | $G_{12}^{CNT}$ (TPa) | $\alpha_{11}^{CNT}$ ($10^{-6}$/K) | $\alpha_{22}^{CNT}$ ($10^{-6}$/K) |
|---|---|---|---|---|---|
| 300 | 5.6466 | 7.0800 | 1.9445 | 3.4584 | 5.1682 |
| 500 | 5.5308 | 6.9348 | 1.9643 | 4.5361 | 5.0189 |
| 700 | 5.4744 | 6.8641 | 1.9644 | 4.6677 | 4.8943 |

### 5.1 Convergence of DQ method

In this section, the convergence of DQ method is appraised by Fig. 2. It can be seen that fast rate of convergence in DQ can be found in this figure, Based on this figure, the sufficient number of grid points to achieve the accurate result is $N$ = 17.

### 5.2 Verification of results

In Table 2, a comparison study is performed to validate the obtained results. For this purpose, a simply supported curved beam with radius of $R$ = 48.34 m, width of $b$ = 5 m, thickness of $h$ = 1.8 m, central angle of $\theta = \pi / 6$, Poisson's ratio of $\nu$ = 0.2 is assumed. The first three dimensionless frequency of the structure is reported in Table 2. As can be seen from Table 2, the present results are in good agreement with the results reported by references (Malekzadeh *et al*. 2010) and Wu and Chiang (2003).

### 5.3 The effect of different parameters

In this section, the effects of different parameters on the frequency and force responses of the curved micro beam under the harmonic transverse centralized force ($x_0 = L/2$) are studied. For parametric study, a CC curved microbeam reinforced by $V_{CNT}^{*}$ = 0.28 CNTs distributed as FGX pattern and subjected to magnetic field with $H_x$ = le8 A/m is considered with the central angle of $\theta = \pi / 6$, width to thickness ratio of $b/h$ = 4, thickness to size parameter ratio of $h / l$ = 2 and temperature of $T$ = 500 $K$.

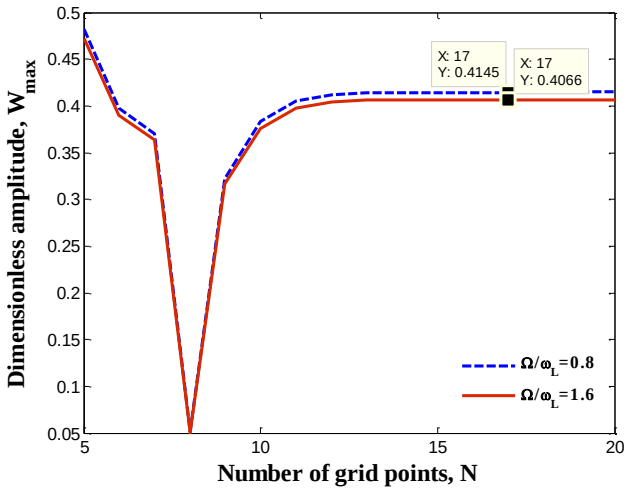


Fig. 2 Convergence and accuracy of DQM

Table 2 Comparison of the first three frequency parameters of the hard simply supported isotropic circular curved beam

| Method | $\Omega_1$ | $\Omega_2$ | $\Omega_3$ |
|---|---|---|---|
| DQM (Malekzadeh *et al*. 2010) | 34.4745 | 137.783 | 299.541 |
| FEM (Wu and Chiang 2003) | 34.543 | 138.019 | 300.285 |
| DQM (Present) | 34.4742 | 137.7815 | 299.5315 |

In Fig. 3 the effect of in-plane and out-of-plane motions on the frequency response and force response of the structure is shown. In this figures, dimensionless maximum deflection and dimensionless forcing amplitude are defined as $W_{\max} = w / h$ and $P = F_0 / A_{11}$ at $T$ = 500 $K$. As can be seen, due to consider the geometric nonlinearity, a hardening-type behavior is observed in the frequency response and force response curves. From Fig. 3(a) it can be

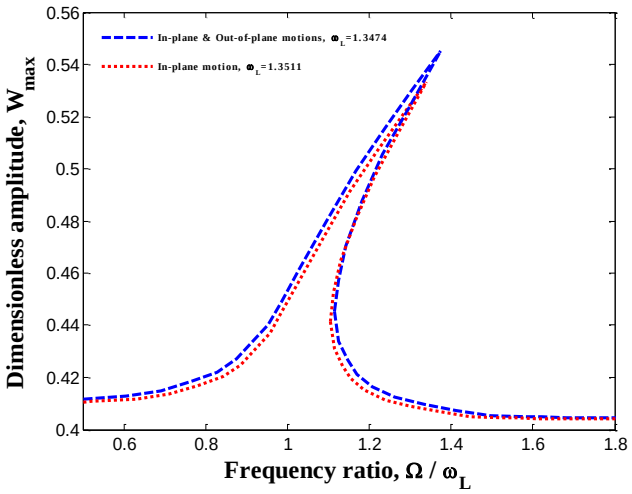


(a)

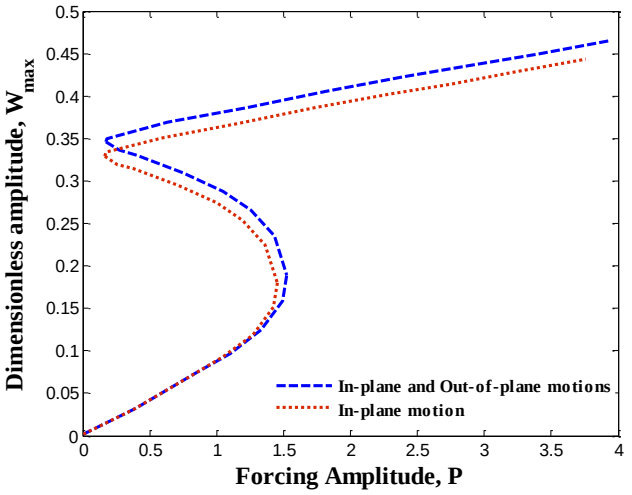


(b)

Fig. 3 Comparison between in-plane and out of plane motions on the (a) frequency response; (b) force response

seen that considering the in-plane and out-of-plane motions together yields the highest dimensionless vibration amplitude with respect to the in-plane motion lonely. Furthermore, the frequency of the structure with only in-plane motion is larger than the structure with in-plane and out-of-plane motions. Also, it can be deduced that the hardening-type response of the structure with in-plane motion is more noticeable with respect to the structure with in-plane and out-of-plane motions. Furthermore, from Fig. 3(b), it can be observed that for lower values of forcing amplitudes, with increasing the forcing amplitude, two limit point bifurcations and a jump phenomenon is happened. Moreover, for properly large values of forcing amplitude, with increasing the forcing amplitude, the maximum vibration amplitude of structure increases.

Fig. 4 illustrates the effect of CNTs distribution types on the frequency and force responses of the nonlinear hardening-type behavior of the structure. It is apparent that the highest frequency and lowest vibration amplitude belongs to FGX distribution type while the inverse condition can be observed for FGO distribution type. Therefore, it can be stated that the hardening-type response of the structure with FGX distribution type is more intense with respect to the other distribution types. Also, the greater amplitude and jump height belongs to the FGO distribution type because the structure with FGO has the lowest stiffness (see Fig. 4 (b)).

The effect of volume fraction of CNTs on the frequency and force responses of the structure is depicted in Fig. 5. It can be found that with increasing the volume fraction of CNTs, the frequency increases while the amplitude peak of the structure decreases (see Fig. 5(a)). Also, from Fig. 5(b) it can be concluded that increasing the CNTs volume fraction decreases the amplitude and jump height and it is due to an increase in the stiffness of the system.

The effect of the central angle of the curved microbeam on the frequency response and force response of the structure is examined by Fig. 6. It is apparent that as the central angle decreases, the frequency increases and as results the vibration amplitude of the curved microbeam decreases and the hardening-type response of the system intensify. Hence, it can be stated that by increasing the

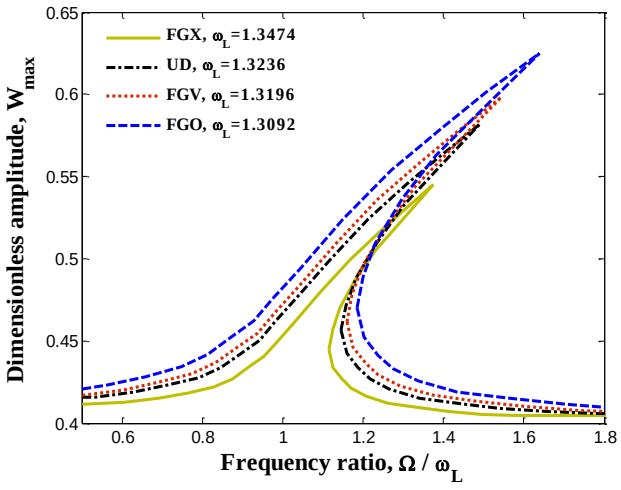


(a)

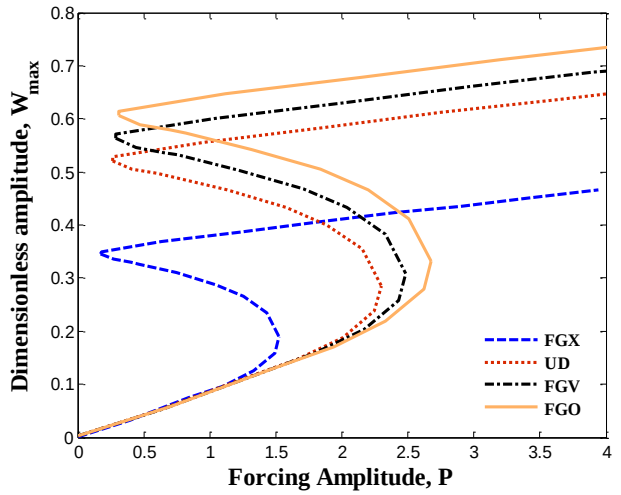


(b)

Fig. 4 The effect of SWCNTs distribution on the (a) frequency response; (b) force response

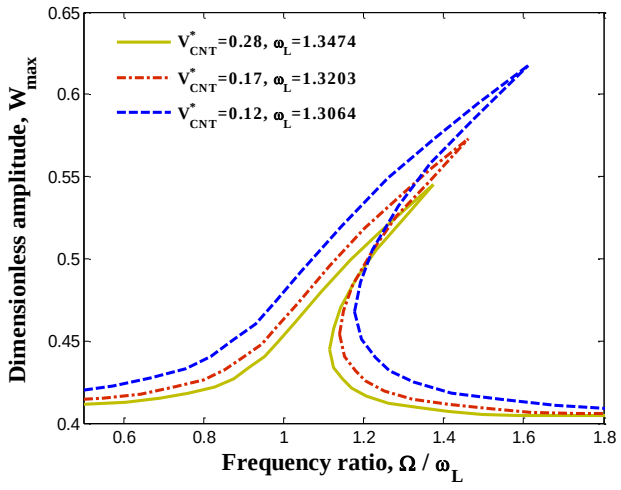


(a)

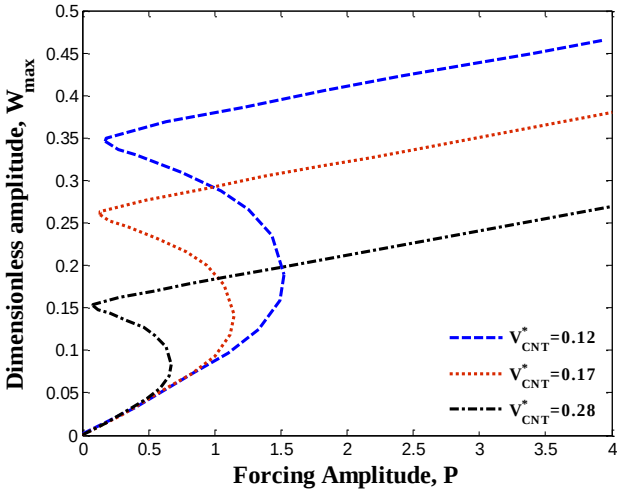


(b)

Fig. 5 The effect of SWCNTs volume percent on the (a) frequency response; (b) force response

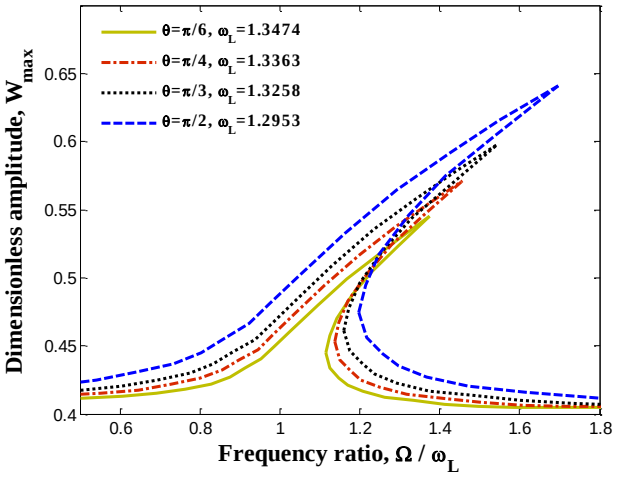


(a)

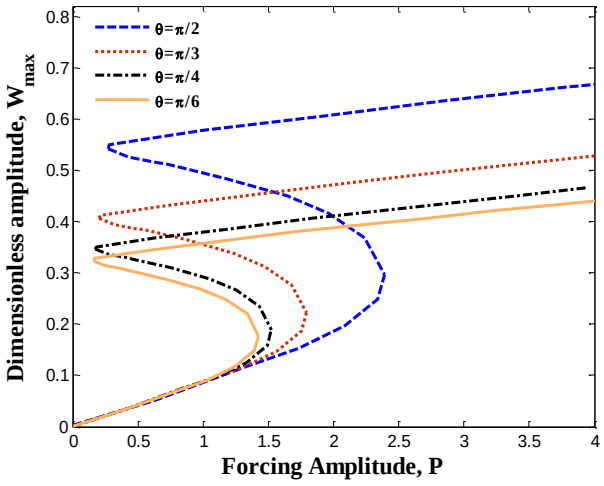


(b)

Fig. 6 The effect of the central angle of the curved microbeam on the (a) frequency response; (b) force response

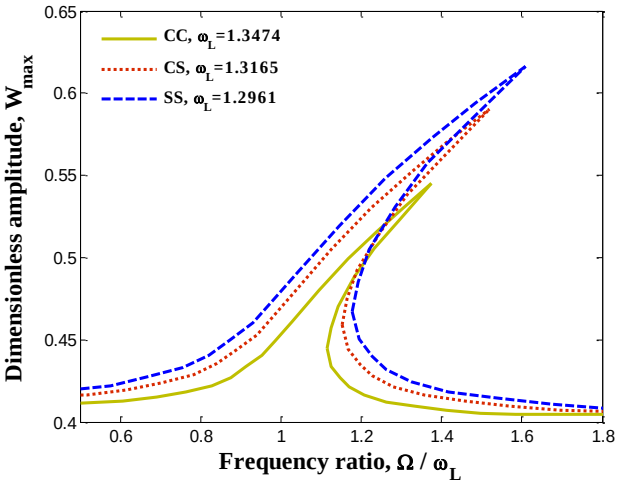


(a)

Fig. 7 The effect of different boundary conditions on the (a) frequency response; (b) force response

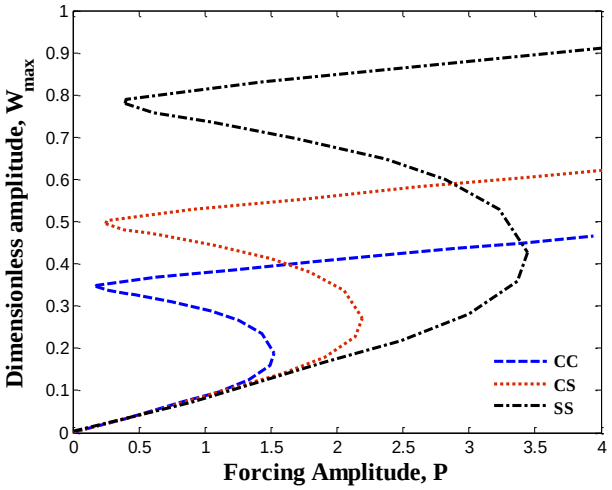


(b)

Fig. 7 Continued

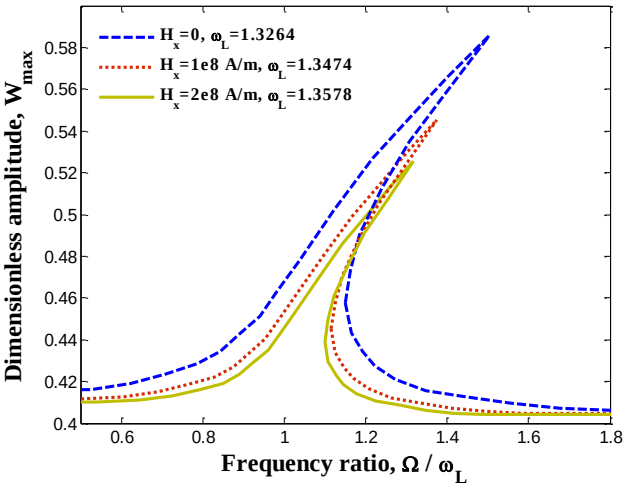


(a)

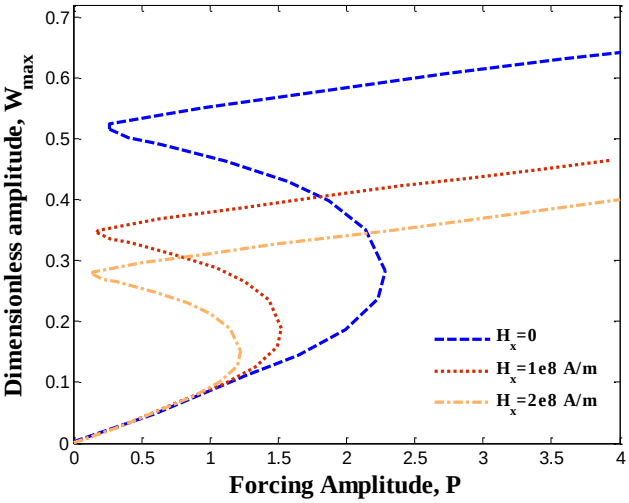


(b)

Fig. 8 The effect of magnetic field on the (a) frequency response; (b) force response

central angle of the curved microbeam, the stiffness of the structure decreases and so the jump height increases.

Fig. 7 shows the effect of various boundary conditions on the frequency and force responses of the system. As can be seen, the maximum frequency and the minimum vibration amplitude belong to the structure with CC boundary condition. It was expectable because the CC boundary condition provides more constraint on the structure and so the stiffness of the system increases. Furthermore, it can be observed that the greater jump height is occurred for SS boundary condition type.

Fig. 8 illustrates the effect of magnetic field of the frequency and force responses of the structure. From this figure, it can be found that applying the magnetic field increases the frequency of the system which is indicative of an increase in the stiffness of the curved microbeam. As a result, by applying the magnetic field the vibration amplitude decreases.

The effect of thickness to material length scale parameter ratio on the behavior of the structure is shown in Fig. 9. It can be deduced that as thickness to material length scale parameter ratio decreases, the frequency of the system increases and the vibration amplitude decreases and consequently the jump height of the structure decreases. On the other word, with increasing the thickness to material length scale parameter ratio, the effect of size-scale becomes less significant and lessens.

From Fig. 10, it can be found that considering the elastic foundation leads to an increase in the stiffness of the system and so the frequency increases. Moreover, the structure with the visco-Pasternak foundation has the lowest vibration amplitude with respect to Winkler foundation. From this figure, it can be stated that the most intense hardening-type response belongs to the structure with visco-Pasternak foundation.

Fig. 11 depicts the effect of temperature change on the frequency response and force response of the curved microbeam. As expected, with increasing temperature the frequency of the structure decreases while the vibration amplitude increases. The reason is that increasing temperature decreases the mechanical properties of the

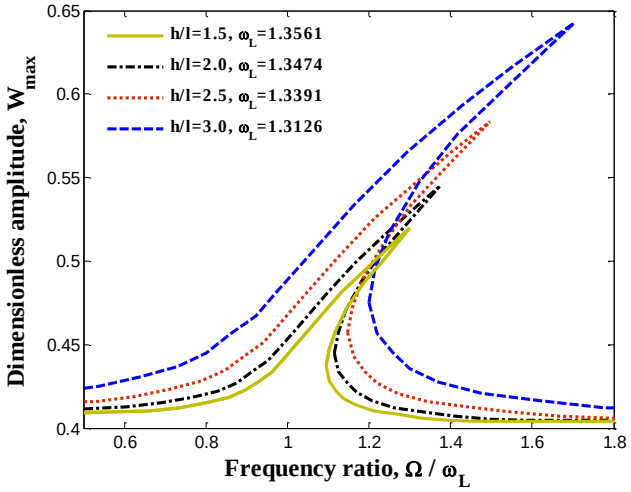


(a)

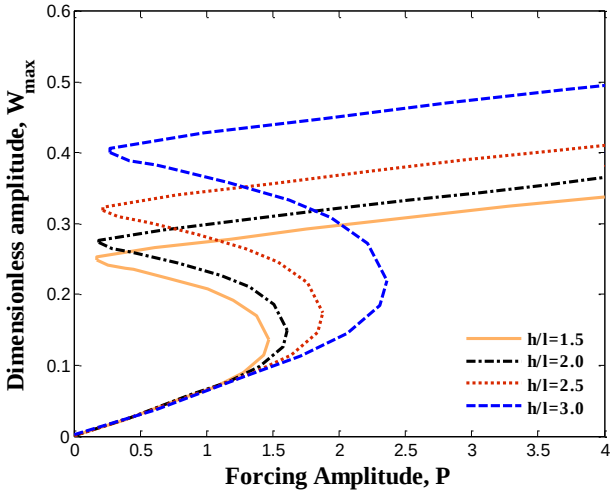


(b)

Fig. 9 The effect of thickness to material length scale parameter ratio on the (a) frequency response; (b) force response

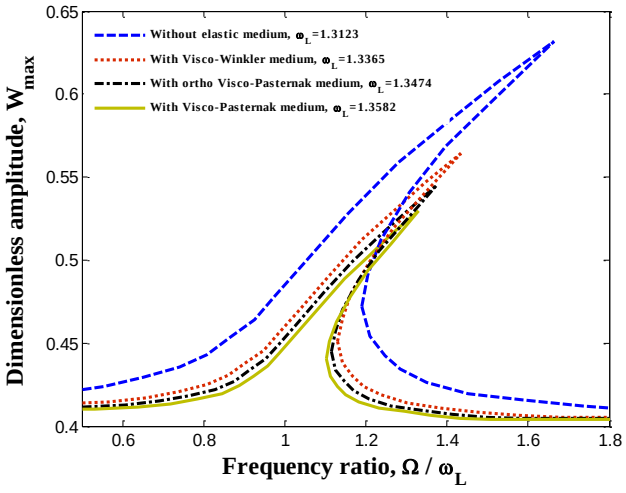


(a)

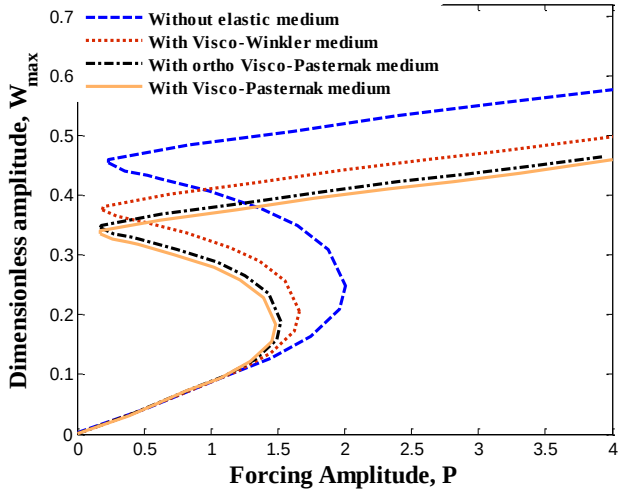


(b)

Fig. 10 The effect of viscoelastic medium type on the (a) frequency response; (b) force response

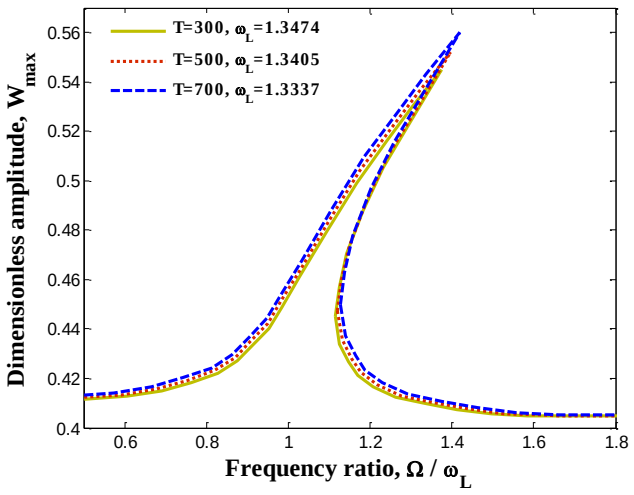


(a)

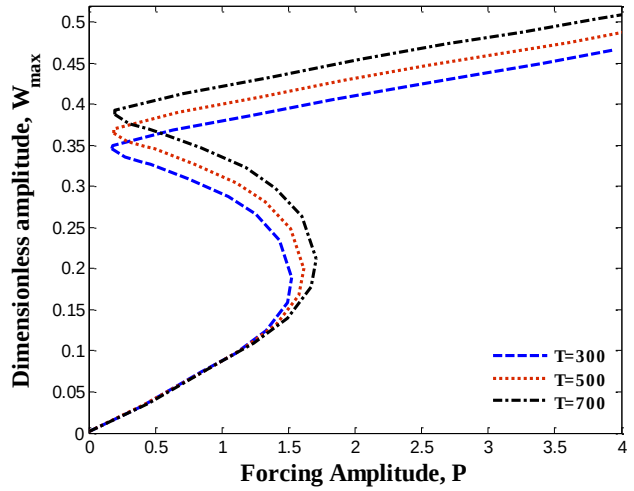


(b)

Fig. 11 The effect of temperature on the (a) frequency response; (b) force response

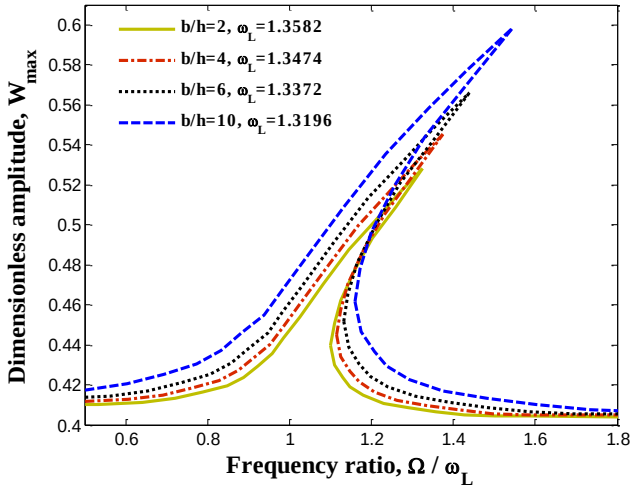


(a)

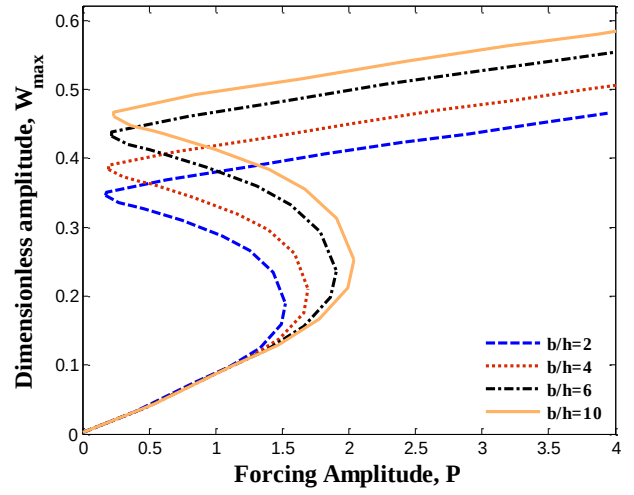


(b)

Fig. 12 The effect of width to thickness ratio on the (a) frequency response; (b) force response

structure and so the stiffness of the system gets smaller. Furthermore, as temperature increases, the jump height of the structure increases.

Fig. 12 illustrates the effect of width to thickness ratio on the frequency and force responses of the structure. As can be seen, with increasing the width to thickness ration, the frequency of the system decreases whilst the amplitude peak increases. The reason is that with increasing the width to thickness ratio, the curved microbeam becomes thinner and so the stiffness of the structure decreases. Therefore, the hardening effects become more noticeable for the structure with lower values of width to thickness ratio.

## 6. Conclusions

In this research, the in-plane and out-of-plane forced vibration of a curved nanocomposite microbeam was analyzed. The in-plane and out-of-plane displacements of the structure were considered based on FSDT. The curved microbeam was reinforced by FG-CNTs and so the extended rule of mixture was employed to estimate the effective material properties of the structure. Also, the small scale effect was taken into account using SGT. The structure was rested by a nonlinear orthotropic viscoelastic foundation and was subjected to concentrated harmonic force, thermal and magnetic loads. The derivation of the governing equations was performed using energy method and Hamilton's principle. DQ method along with IQ and Newmark methods were employed to solve the problem. The most important results may be listed as follows

- The highest frequency and lowest vibration amplitude belongs to FGX distribution type while the inverse condition is observed for FGO distribution type. Thus, it can be stated that the hardening-type response of the structure with FGX distribution type is more intense with respect to the other distribution types.
- With increasing the volume fraction of CNTs, the frequency increases while the amplitude peak of the structure decreases. Furthermore, it is concluded that

increasing the CNTs volume fraction decreases the amplitude and jump height and it is due to an increase in the stiffness of the system.

- As the central angle decreases, the frequency increases and as a results the vibration amplitude of the curved microbeam decreases.
- Comparing the effect of boundary condition, the higher frequency and the lower vibration amplitude belong to the structure with CC boundary condition. Furthermore, it is seen that the greater jump height is occurred for SS boundary condition type.
- Applying the magnetic field increases the frequency of the system which is indicative of an increase in the stiffness of the curved microbeam. As a result, by applying the magnetic field the vibration amplitude decreases.
- It is deduced that as thickness to material length scale parameter ratio decreases, the frequency of the system increases and the vibration amplitude decreases and consequently the jump height of the structure decreases.
- With increasing the width to thickness ratio, the frequency of the system decreases whilst the amplitude peak increases.

## References


Atcı, D. and Bağdatlı, S.M. (2017a), "Free vibrations of fluid conveying microbeams under non-ideal boundary conditions", *Steel Compos. Struct., Int. J.*, **24**(2), 141-149.

Atcı, D. and Bağdatlı, S.M. (2017b), "Vibrations of fluid conveying microbeams under non-ideal boundary conditions", *Microsyst. Technol.*, **23**(10), 4741-4752.

Allahkarami, F. and Nikkhah-bahrami, M. (2017), "Effects of agglomerated CNTs as reinforcement on the size-dependent vibration of embedded curved microbeams based on the modified couple stress theory", *Mech. Adv. Mat. Struct.*, 1-14.

Allahkarami, F., Nikkhah-bahrami, M. and Ghassabzadeh Saryazdi, M. (2017), "Magneto-thermo-mechanical dynamic buckling analysis of a FG-CNTs-reinforced curved microbeam with different boundary conditions using strain gradient theory", *Int. J. Mech. Mater. Des.*, 1-19.

~~Aydin~~ Aya, S.A. and Tufekci, E. (2017), "Modeling and analysis of out-of-plane behavior of curved nanobeams based on nonlocal elasticity", *Compos. Part B: Eng.*, **119**, 184-195.

Bataineh, A.M. and Younis, M.I. (2015), "Dynamics of a clamped–clamped microbeam resonator considering fabrication imperfections", *Microsyst. Technol.*, **21**(11), 2425-2434.

Dai, H.L., Wang, Y.K. and Wang, L. (2015), "Nonlinear dynamics of cantilevered microbeams based on modified couple stress theory", *Int. J. Eng. Sci.*, **94**, 103-112.

Dehrouyeh-Semnani, A.M., Dehrouyeh, M., Zafari-Koloukhi, H. and Ghamami, M. (2015), "Size-dependent frequency and stability characteristics of axially moving microbeams based on modified couple stress theory", *Int. J. Eng. Sci.*, **97**, 98-112.

Dehrouyeh-Semnani, A.M., Mostafaei, H. and Nikkhah-Bahrami, M. (2016), "Free flexural vibration of geometrically imperfect functionally graded microbeams", *Int. J. Eng. Sci.*, **105**, 56-79.

Erfani, S. and Akrami, V. (2016), "Evaluation of cyclic fracture in perforated beams using micromechanical fatigue model", *Steel Compos. Struct., Int. J.*, **20**(4), 913-930.

Ghayesh, M.H. and Farokhi, H. (2017), "Global dynamics of imperfect axially forced microbeams", *Int. J. Eng. Sci.*, **115**, 102-116.

Ghayesh, M.H., Farokhi, H. and Gholipour, A. (2017), "Coupled vibrations of functionally graded Timoshenko microbeams", *Europ. J. Mech. A/Solids*, **65**, 289-300.

Gutschmidt, S. and Gottlieb, O. (2012), "Nonlinear dynamic behavior of a microbeam array subject to parametric actuation at low, medium and large DC-voltages", *Nonlinear. Dyn.*, **67**(1), 1-36.

He, X.j., Wu, Q., Wang, Y., Song, M.x. and Yin, J.h. (2009), "Numerical simulation and analysis of electrically actuated microbeam-based MEMS capacitive switch", *Microsyst. Technol.*, **15**(2), 301-307.

Jafari-Talookolaei, R.A., Abedi, M. and Attar, M. (2017), "In-plane and out-of-plane vibration modes of laminated composite beams with arbitrary lay-ups", *Aerosp. Sci. Tech.*, **66**, 366-379.

Jahangiri, R., Jahangiri, H. and Khezerloo, H. (2015), "FGM micro-gripper under electrostatic and intermolecular Van-der Waals forces using modified couple stress theory", *Steel Compos. Struct., Int. J.*, **18**(6), 1541-1555.

Kolahchi, R. (2017~~b~~), "A comparative study on the bending vibration and buckling of viscoelastic sandwich nano-plates based on different nonlocal theories using DC HDQ and DQ methods", *Aerosp. Sci. Tech.*, **66**, 235-248.

Kolahchi, R. and Moniribidgoli, A.M. (2016), "Size-dependent sinusoidal beam model for dynamic instability of single-walled carbon nanotubes", *Appl. Math. Mech. -Engl Ed*, **37**(2), 265-274.

Kolahchi, R., Rabani Bidgoli, M., Beygipoor, Gh. and Fakhar, M.H. (2015), "A nonlocal nonlinear analysis for buckling in embedded FG-SWCNT-reinforced microplates subjected to magnetic field", *J. Mech. Sci. Tech.*, **29**(9), 3669-3677.

Kolahchi, R., Hosseini, H. and Esmailpour, M. (2016a), "Differential cubature and quadrature-Bolotin methods for dynamic stability of embedded piezoelectric nanoplates based on visco-nonlocal-piezoelasticity theories", *Compos. Struct.*, **157**, 174-186.

Kolahchi, R., Hosseini, H. and Esmailpour, M. (2016b), "Dynamic stability analysis of temperature-dependent functionally graded CNT-reinforced visco-plates resting on orthotropic elastomeric medium", *Compos. Struct.*, **150**, 255-265.

Kolahchi, R., Zarei, M.Sh., Hajmohammad, M.H. and Naddaf Oskouei, A. (2017~~a~~), "Visco-nonlocal-refined Zigzag theories for dynamic buckling of laminated nanoplates using differential cubature-Bolotin methods", *Thin-Wall. Struct.*, **113**, 162-169.

Krylov, S., Ilic, B.R. and Lulinsky, S. (2011), "Bistability of curved microbeams actuated by fringing electrostatic fields", *Nonlinear Dyn.*, **66**(3), 403-411.

Liu, B., Xing, Y., Wang, Z., Lu, X. and Sun, H. (2017), "Non-uniform rational Lagrange functions and its applications to isogeometric analysis of in-plane and flexural vibration of thin plates", *Comput. Meth Appl. Mech. Eng.*, **321**, 173-208.

Malekzadeh, P., Golbahar Haghighi, M.R. and Atashi, M.M. (2010), "Out-of-plane free vibration of functionally graded circular curved beams in thermal environment", *Compos. Struct.* **92**(2), 541-552 .

Pan, F., Chen, Y., Liu, Y. and Guo, Z. (2017), "Out-of-plane bending of carbon nanotube films", *Int. J. Solids Struct.*, **106-107**, 183-199.

Peng, J., Yang, L., Lin, F. and Yang, J. (2017), "Dynamic analysis of size-dependent micro-beams with nonlinear elasticity under electrical actuation", *Appl. Math. Model.*, **43**, 441-453.

Rezaei, M.P. and Zamanian, M. (2017), "A two-dimensional vibration analysis of piezoelectrically actuated microbeam with nonideal boundary conditions", *Physica E*, **85**, 285-293.

Rostami, H., Rahbar Ranji, A. and Bakhtiarinejad, F. (2016), "Free in-plane vibration analysis of rotating rectangular orthotropic cantilever plates", *Int. J. Mech. Sci.*, **115~~-116~~**, 438-456.

Shafiei, N., Kazemi, M. and Ghadiri, M. (2016), "Nonlinear vibration of axially functionally graded tapered microbeams", *Int. J. Eng. Sci.*, **102**, 12-26.

Shen, H.Sh. (2009), "Nonlinear bending of functionally graded carbon nanotube-reinforced composite plates in thermal environments", *Compos. Struct.*, **91**(1), 9-19.

Shen, H.Sh. and Zhang, Ch.L. (2011), "Nonlocal beam model for nonlinear analysis of carbon nanotubes on elastomeric substrates", *Comput. Mat. Sci.*, **50**(3), 1022-1029.

Shu, C., Chew, Y.T. and Richards, E. (1995), "Generalized differential and integral quadrature and their application to solve boundary layer equations", *Int. J. Num. Meth. Fluids*, **21**(9), 723-733.

Simsek, M. and Kocaturk, T. (2009), "Nonlinear dynamic analysis of an eccentrically prestressed damped beam under a concentrated moving harmonic load", *J. Sound Vib.*, **320**(1-2), 235-253.

Wang, Ch., Ayalew, B., Rhyne, T., Cron, S. and Daolliez, B. (2016), "Forced in-plane vibration of a thick ring on a unilateral elastic foundation", *J. Sound Vib.*, **380**, 279-294.

Wu, J.S. and Chiang, L.K. (2003), "Out-of-plane response of a circular Timoshenko beam due to moving load", *Int. J. Solids Struct.*, **40**(26), 7425-7448.

Younis, M.I. and Nayfeh, A.H. (2003), "A study of the nonlinear response of a resonant microbeam to an electric actuation", *Nonlinear Dyn.*, **31**(1), 91-117.

Zhang, B., He, Y., Liu, D., Gan, Zh. and Shen, L. (2013), "A novel size-dependent functionally graded curved mircobeam model based on the strain gradient elasticity theory", *Compos. Struct.*, **106**, 374-392.

*CC*

## Appendix A

$$N_x = \int_s \sigma_{xx} dA = A_{11}\frac{\partial u}{\partial x} + A_{11}\frac{w}{R} + B_{11}\frac{\partial \varphi_y}{\partial x} + C_{11}\left(\frac{\varphi_x}{R} - \frac{\partial \varphi_z}{\partial x}\right) + \frac{1}{2}A_{11}\left(\frac{\partial v}{\partial x}\right)^2 + \frac{1}{2}A_{11}\left(\frac{\partial w}{\partial x}\right)^2 - \tilde{A}_{11}\Delta T \tag{A1}$$

$$M_x^1 = \int_s \sigma_{xx} z dA = B_{11}\frac{\partial u}{\partial x} + B_{11}\frac{w}{R} + D_{11}\frac{\partial \varphi_y}{\partial x} + \frac{1}{2}B_{11}\left(\frac{\partial v}{\partial x}\right)^2 + \frac{1}{2}B_{11}\left(\frac{\partial w}{\partial x}\right)^2 - \tilde{B}_{11}\Delta T \tag{A2}$$

$$M_x^2 = \int_s \sigma_{xx} y dA = C_{11}\frac{\partial u}{\partial x} + C_{11}\frac{w}{R} + F_{11}\left(\frac{\varphi_x}{R} - \frac{\partial \varphi_z}{\partial x}\right) + \frac{1}{2}C_{11}\left(\frac{\partial v}{\partial x}\right)^2 + \frac{1}{2}C_{11}\left(\frac{\partial w}{\partial x}\right)^2 - \tilde{C}_{11}\Delta T \tag{A3}$$

$$Q_{xz} = \int_s \tau_{xz} dA = k_s \begin{pmatrix} A_{22}\frac{\partial w}{\partial x} - A_{22}\frac{u}{R} - A_{22}\varphi_y \\ -\frac{1}{R}B_{22}\varphi_y + C_{22}\left(\frac{\varphi_z}{R} - \frac{\partial \varphi_x}{\partial x}\right) \end{pmatrix} \tag{A4}$$

$$P_{xz}^1 = \int_s \tau_{xz} z dA = B_{22}\frac{\partial w}{\partial x} - B_{22}\frac{u}{R} - B_{22}\varphi_y - \frac{1}{R}D_{22}\varphi_y \tag{A5}$$

$$P_{xz}^2 = \int_s \tau_{xz} y dA = C_{22}\frac{\partial w}{\partial x} - C_{22}\frac{u}{R} - C_{22}\varphi_y + F_{22}\left(\frac{\varphi_z}{R} - \frac{\partial \varphi_x}{\partial x}\right) \tag{A6}$$

$$Q_{xy} = \int_s \tau_{xz} dA = k_s\left(A_{22}\frac{\partial v}{\partial x} - A_{22}\varphi_z - B_{22}\frac{\partial \varphi_x}{\partial x}\right) \tag{A7}$$

$$P_{xy} = \int_s \tau_{xz} z dA = B_{22}\frac{\partial v}{\partial x} - B_{22}\varphi_z - D_{22}\frac{\partial \varphi_x}{\partial x} \tag{A8}$$

$$P_x = \int_s p_x dA = 2l_0^2\left(A_{22}\frac{\partial^2 u}{\partial x^2} + \frac{1}{R}A_{22}\frac{\partial w}{\partial x} + B_{22}\frac{\partial^2 \varphi_y}{\partial x^2} + C_{22}\left(\frac{1}{R}\frac{\partial \varphi_x}{\partial x} - \frac{\partial^2 \varphi_z}{\partial x^2}\right) + A_{22}\frac{\partial v}{\partial x}\frac{\partial^2 v}{\partial x^2} + A_{22}\frac{\partial w}{\partial x}\frac{\partial^2 w}{\partial x^2}\right) \tag{A9}$$

$$S_x^1 = \int_s p_x z dA = 2l_0^2\left(B_{22}\frac{\partial^2 u}{\partial x^2} + \frac{1}{R}B_{22}\frac{\partial w}{\partial x} + D_{22}\frac{\partial^2 \varphi_y}{\partial x^2} + B_{22}\frac{\partial v}{\partial x}\frac{\partial^2 v}{\partial x^2} + B_{22}\frac{\partial w}{\partial x}\frac{\partial^2 w}{\partial x^2}\right) \tag{A10}$$

$$S_x^2 = \int_s p_x y dA = 2l_0^2\left(C_{22}\frac{\partial^2 u}{\partial x^2} + \frac{1}{R}C_{22}\frac{\partial w}{\partial x} + F_{22}\left(\frac{1}{R}\frac{\partial \varphi_x}{\partial x} - \frac{\partial^2 \varphi_z}{\partial x^2}\right) + C_{22}\frac{\partial v}{\partial x}\frac{\partial^2 v}{\partial x^2} + C_{22}\frac{\partial w}{\partial x}\frac{\partial^2 w}{\partial x^2}\right) \tag{A11}$$

$$P_y = \int_s p_y dA = 2l_0^2\left(\frac{1}{R}A_{22}\varphi_x - A_{22}\frac{\partial \varphi_z}{\partial x}\right) \tag{A12}$$

$$P_z = \int_s p_z dA = 2l_0^2 A_{22}\frac{\partial \varphi_y}{\partial x} \tag{A13}$$

$$Y_x = \int_s m_{xx} dA = 2l_2^2\begin{pmatrix} A_{22}\frac{\partial \varphi_x}{\partial x} - \frac{1}{R}B_{22}\frac{\partial \varphi_x}{\partial x} \\ +\frac{1}{2R}A_{22}\left(\frac{\partial v}{\partial x} + \varphi_z\right) \end{pmatrix} \tag{A14}$$

$$X_x = \int_s m_{xx} z dA = 2l_2^2\begin{pmatrix} B_{22}\frac{\partial \varphi_x}{\partial x} - \frac{1}{R}D_{22}\frac{\partial \varphi_x}{\partial x} \\ +\frac{1}{2R}B_{22}\left(\frac{\partial v}{\partial x} + \varphi_z\right) \end{pmatrix} \tag{A15}$$

$$Y_y = \int_s m_{yy} dA = -l_2^2 A_{22}\left(\frac{\partial \varphi_x}{\partial x} + \frac{\varphi_z}{R}\right) \tag{A16}$$

$$Y_z = \int_s m_{zz} dA = -l_2^2 A_{22}\frac{\partial \varphi_x}{\partial x} \tag{A17}$$

$$Y_{xy} = \int_s m_{xy} dA = \frac{l_2^2}{2}\left(A_{22}\frac{\partial \varphi_y}{\partial x} - A_{22}\frac{\partial^2 w}{\partial x^2} + \frac{1}{R}A_{22}\frac{\partial u}{\partial x} - C_{22}\frac{\partial^2 \varphi_x}{\partial x^2} + \frac{1}{R}B_{22}\frac{\partial \varphi_y}{\partial x} - \frac{1}{R}C_{22}\frac{\partial \varphi_z}{\partial x}\right) \tag{A18}$$

$$X_{xy}^1 = \int_s m_{xy} z dA = \frac{l_2^2}{2}\left(B_{22}\frac{\partial \varphi_y}{\partial x} - B_{22}\frac{\partial^2 w}{\partial x^2} + \frac{1}{R}B_{22}\frac{\partial u}{\partial x} + \frac{1}{R}D_{22}\frac{\partial \varphi_y}{\partial x}\right) \tag{A19}$$

$$X_{xy}^2 = \int_s m_{xy} y dA = \frac{l_2^2}{2}\left(C_{22}\frac{\partial \varphi_y}{\partial x} - C_{22}\frac{\partial^2 w}{\partial x^2} + \frac{1}{R}C_{22}\frac{\partial u}{\partial x} - F_{22}\frac{\partial^2 \varphi_x}{\partial x^2} - \frac{1}{R}F_{22}\frac{\partial \varphi_z}{\partial x}\right) \tag{A20}$$

$$Y_{xz}=\int_s m_{xz}dA=\frac{l_2^2}{2}\left(\begin{array}{l}A_{22}\dfrac{\partial^2 v}{\partial x^2}+A_{22}\dfrac{\partial \varphi_z}{\partial x}\\ -B_{22}\dfrac{\partial^2 \varphi_x}{\partial x^2}-\dfrac{2}{R}A_{22}\varphi_x\end{array}\right) \tag{A21}$$

$$X_{xz}=\int_s m_{xz}zdA=\frac{l_2^2}{2}\left(\begin{array}{l}B_{22}\dfrac{\partial^2 v}{\partial x^2}+B_{22}\dfrac{\partial \varphi_z}{\partial x}\\ -D_{22}\dfrac{\partial^2 \varphi_x}{\partial x^2}-\dfrac{2}{R}B_{22}\varphi_x\end{array}\right) \tag{A22}$$

$$Y_{yz}=\int_s m_{yz}dA=\frac{l_2^2}{2R}A_{22}\varphi_y \tag{A23}$$

$$\begin{aligned}T_{xxx}=\int_s \tau_{xxx}^{(1)}dA=\frac{4}{5}l_1^2\Bigg(&A_{22}\frac{\partial^2 u}{\partial x^2}+\frac{1}{R}A_{22}\frac{\partial w}{\partial x}\\ &+A_{22}\frac{\partial v}{\partial x}\frac{\partial^2 v}{\partial x^2}+A_{22}\frac{\partial w}{\partial x}\frac{\partial^2 w}{\partial x^2}+\frac{1}{2R}A_{22}\varphi_y\\ &+B_{22}\frac{\partial^2 \varphi_y}{\partial x^2}+C_{22}\left(\frac{1}{R}\frac{\partial \varphi_x}{\partial x}-\frac{\partial^2 \varphi_z}{\partial x^2}\right)\Bigg)\end{aligned} \tag{A24}$$

$$\begin{aligned}M_{xxx}^{1}=\int_s \tau_{xxx}^{(1)}zdA=\frac{4}{5}l_1^2\Bigg(&B_{22}\frac{\partial^2 u}{\partial x^2}+\frac{1}{R}B_{22}\frac{\partial w}{\partial x}\\ &+B_{22}\frac{\partial v}{\partial x}\frac{\partial^2 v}{\partial x^2}+B_{22}\frac{\partial w}{\partial x}\frac{\partial^2 w}{\partial x^2}+\frac{1}{2R}B_{22}\varphi_y+D_{22}\frac{\partial^2 \varphi_y}{\partial x^2}\Bigg)\end{aligned} \tag{A25}$$

$$\begin{aligned}M_{xxx}^{2}=\int_s \tau_{xxx}^{(1)}ydA=\frac{4}{5}l_1^2\Bigg(&C_{22}\frac{\partial^2 u}{\partial x^2}+\frac{1}{R}C_{22}\frac{\partial w}{\partial x}\\ &+C_{22}\frac{\partial v}{\partial x}\frac{\partial^2 v}{\partial x^2}+C_{22}\frac{\partial w}{\partial x}\frac{\partial^2 w}{\partial x^2}+\frac{1}{2R}C_{22}\varphi_y\\ &+F_{22}\left(\frac{1}{R}\frac{\partial \varphi_x}{\partial x}-\frac{\partial^2 \varphi_z}{\partial x^2}\right)\Bigg)\end{aligned} \tag{A26}$$

$$\begin{aligned}T_{yyy}=\int_s \tau_{yyy}^{(1)}dA=-\frac{2}{3}l_1^2\Bigg(&A_{22}\frac{\varphi_x}{R}-2A_{22}\frac{\partial \varphi_z}{\partial x}\\ &+A_{22}\frac{\partial^2 v}{\partial x^2}-B_{22}\frac{\partial^2 \varphi_x}{\partial x^2}\Bigg)\end{aligned} \tag{A27}$$

$$\begin{aligned}M_{yyy}=\int_s \tau_{yyy}^{(1)}zdA=-\frac{2}{3}l_1^2\Bigg(&B_{22}\frac{\varphi_x}{R}-2B_{22}\frac{\partial \varphi_z}{\partial x}\\ &+B_{22}\frac{\partial^2 v}{\partial x^2}-D_{22}\frac{\partial^2 \varphi_x}{\partial x^2}\Bigg)\end{aligned} \tag{A28}$$

$$\begin{aligned}T_{zzz}=\int_s \tau_{zzz}^{(1)}dA=-\frac{2}{5}l_1^2\Bigg(&2A_{22}\frac{\partial \varphi_y}{\partial x}+A_{22}\frac{\partial^2 w}{\partial x^2}\\ &-\frac{1}{R}A_{22}\frac{\partial u}{\partial x}+C_{22}\left(\frac{1}{R}\frac{\partial \varphi_z}{\partial x}-\frac{\partial^2 \varphi_x}{\partial x^2}\right)-\frac{1}{R}B_{22}\frac{\partial \varphi_y}{\partial x}\Bigg)\end{aligned} \tag{A29}$$

$$\begin{aligned}M_{zzz}^{1}=\int_s \tau_{zzz}^{(1)}zdA=-\frac{2}{5}l_1^2\Bigg(&2B_{22}\frac{\partial \varphi_y}{\partial x}\\ &+B_{22}\frac{\partial^2 w}{\partial x^2}-\frac{1}{R}B_{22}\frac{\partial u}{\partial x}-\frac{1}{R}D_{22}\frac{\partial \varphi_y}{\partial x}\Bigg)\end{aligned} \tag{A30}$$

$$\begin{aligned}M_{zzz}^{2}=\int_s \tau_{zzz}^{(1)}ydA=-\frac{2}{5}l_1^2\Bigg(&2C_{22}\frac{\partial \varphi_y}{\partial x}+C_{22}\frac{\partial^2 w}{\partial x^2}\\ &-\frac{1}{R}C_{22}\frac{\partial u}{\partial x}+F_{22}\left(\frac{1}{R}\frac{\partial \varphi_z}{\partial x}-\frac{\partial^2 \varphi_x}{\partial x^2}\right)\Bigg)\end{aligned} \tag{A31}$$

$$T_{xyz}=\int_s \tau_{xyz}^{(1)}dA=\frac{1}{3}l_1^2\left(A_{22}\frac{\varphi_z}{R}-2A_{22}\frac{\partial \varphi_x}{\partial x}\right) \tag{A32}$$

$$\begin{aligned}T_{xxy}=\int_s \tau_{xxy}^{(1)}dA=\frac{8}{5}l_1^2\Bigg(&A_{22}\frac{\varphi_x}{R}-2A_{22}\frac{\partial \varphi_z}{\partial x}\\ &+A_{22}\frac{\partial^2 v}{\partial x^2}-B_{22}\frac{\partial^2 \varphi_x}{\partial x^2}\Bigg)\end{aligned} \tag{A33}$$

$$\begin{aligned}M_{xxy}=\int_s \tau_{xxy}^{(1)}zdA=\frac{8}{5}l_1^2\Bigg(&B_{22}\frac{\varphi_x}{R}\\ &-2B_{22}\frac{\partial \varphi_z}{\partial x}+B_{22}\frac{\partial^2 v}{\partial x^2}-D_{22}\frac{\partial^2 \varphi_x}{\partial x^2}\Bigg)\end{aligned} \tag{A34}$$

$$\begin{aligned}T_{xxz}=\int_s \tau_{xxz}^{(1)}dA=\frac{8}{15}l_1^2\Bigg(&2A_{22}\frac{\partial \varphi_y}{\partial x}+A_{22}\frac{\partial^2 w}{\partial x^2}\\ &-\frac{1}{R}A_{22}\frac{\partial u}{\partial x}+C_{22}\left(\frac{1}{R}\frac{\partial \varphi_z}{\partial x}-\frac{\partial^2 \varphi_x}{\partial x^2}\right)\\ &-\frac{1}{R}B_{22}\frac{\partial \varphi_y}{\partial x}\Bigg)\end{aligned} \tag{A35}$$

$$\begin{aligned}M_{xxz}^{1}=\int_s \tau_{xxz}^{(1)}zdA=\frac{8}{15}l_1^2\Bigg(&2B_{22}\frac{\partial \varphi_y}{\partial x}+B_{22}\frac{\partial^2 w}{\partial x^2}\\ &-\frac{1}{R}B_{22}\frac{\partial u}{\partial x}-\frac{1}{R}D_{22}\frac{\partial \varphi_y}{\partial x}\Bigg)\end{aligned} \tag{A36}$$

$$\begin{aligned}M_{xxz}^{2}=\int_s \tau_{xxz}^{(1)}ydA=\frac{8}{15}l_1^2\Bigg(&2C_{22}\frac{\partial \varphi_y}{\partial x}+C_{22}\frac{\partial^2 w}{\partial x^2}\\ &-\frac{1}{R}C_{22}\frac{\partial u}{\partial x}+F_{22}\left(\frac{1}{R}\frac{\partial \varphi_z}{\partial x}-\frac{\partial^2 \varphi_x}{\partial x^2}\right)\Bigg)\end{aligned} \tag{A37}$$

$$\begin{aligned}T_{yyx}=\int_s \tau_{yyx}^{(1)}dA=-\frac{2}{5}l_1^2\Bigg(&A_{22}\frac{\partial^2 u}{\partial x^2}+\frac{1}{R}A_{22}\frac{\partial w}{\partial x}\\ &+A_{22}\frac{\partial v}{\partial x}\frac{\partial^2 v}{\partial x^2}+A_{22}\frac{\partial w}{\partial x}\frac{\partial^2 w}{\partial x^2}+B_{22}\frac{\partial^2 \varphi_y}{\partial x^2}\\ &+C_{22}\left(\frac{1}{R}\frac{\partial \varphi_x}{\partial x}-\frac{\partial^2 \varphi_z}{\partial x^2}\right)\Bigg)+\frac{2}{15R}l_1^2A_{22}\varphi_y\end{aligned} \tag{A38}$$

$$M^{1}_{yyx}=\int_s \tau^{(1)}_{yyx} z dA=-\frac{2}{5}l_1^2\left(B_{22}\frac{\partial^2 u}{\partial x^2}+\frac{1}{R}B_{22}\frac{\partial w}{\partial x}+B_{22}\frac{\partial v}{\partial x}\frac{\partial^2 v}{\partial x^2}+B_{22}\frac{\partial w}{\partial x}\frac{\partial^2 w}{\partial x^2}+D_{22}\frac{\partial^2 \varphi_y}{\partial x^2}\right)+\frac{2}{15R}l_1^2 B_{22}\varphi_y \tag{A39}$$

$$M^{2}_{yyx}=\int_s \tau^{(1)}_{yyx} y dA=-\frac{2}{5}l_1^2\left(C_{22}\frac{\partial^2 u}{\partial x^2}+\frac{1}{R}C_{22}\frac{\partial w}{\partial x}+C_{22}\frac{\partial v}{\partial x}\frac{\partial^2 v}{\partial x^2}+C_{22}\frac{\partial w}{\partial x}\frac{\partial^2 w}{\partial x^2}+F_{22}\left(\frac{1}{R}\frac{\partial \varphi_x}{\partial x}-\frac{\partial^2 \varphi_z}{\partial x^2}\right)\right)+\frac{2}{15R}l_1^2 C_{22}\varphi_y \tag{A40}$$

$$T_{yyz}=\int_s \tau^{(1)}_{yyz} dA=-\frac{2}{15}l_1^2\left(2A_{22}\frac{\partial \varphi_y}{\partial x}+A_{22}\frac{\partial^2 w}{\partial x^2}-\frac{1}{R}A_{22}\frac{\partial u}{\partial x}+C_{22}\left(\frac{1}{R}\frac{\partial \varphi_z}{\partial x}-\frac{\partial^2 \varphi_x}{\partial x^2}\right)-\frac{1}{R}B_{22}\frac{\partial \varphi_y}{\partial x}\right) \tag{A41}$$

$$M^{1}_{yyz}=\int_s \tau^{(1)}_{yyz} z dA=-\frac{2}{15}l_1^2\left(2B_{22}\frac{\partial \varphi_y}{\partial x}+B_{22}\frac{\partial^2 w}{\partial x^2}-\frac{1}{R}B_{22}\frac{\partial u}{\partial x}-\frac{1}{R}D_{22}\frac{\partial \varphi_y}{\partial x}\right) \tag{A42}$$

$$M^{2}_{yyz}=\int_s \tau^{(1)}_{yyz} y dA=-\frac{2}{15}l_1^2\left(2C_{22}\frac{\partial \varphi_y}{\partial x}+C_{22}\frac{\partial^2 w}{\partial x^2}-\frac{1}{R}C_{22}\frac{\partial u}{\partial x}+F_{22}\left(\frac{1}{R}\frac{\partial \varphi_z}{\partial x}-\frac{\partial^2 \varphi_x}{\partial x^2}\right)\right) \tag{A43}$$

$$T_{zzx}=\int_s \tau^{(1)}_{zzx} dA=-\frac{2}{5}l_1^2\left(A_{22}\frac{\partial^2 u}{\partial x^2}+\frac{1}{R}A_{22}\frac{\partial w}{\partial x}+A_{22}\frac{\partial w}{\partial x}\frac{\partial^2 w}{\partial x^2}+A_{22}\frac{\partial v}{\partial x}\frac{\partial^2 v}{\partial x^2}-\frac{8}{15}l_1^2 A_{22}\varphi_y+B_{22}\frac{\partial^2 \varphi_y}{\partial x^2}+C_{22}\left(\frac{1}{R}\frac{\partial \varphi_x}{\partial x}-\frac{\partial^2 \varphi_z}{\partial x^2}\right)\right) \tag{A44}$$

$$M^{1}_{zzx}=\int_s \tau^{(1)}_{zzx} z dA=-\frac{2}{5}l_1^2\left(B_{22}\frac{\partial^2 u}{\partial x^2}+\frac{1}{R}B_{22}\frac{\partial w}{\partial x}+B_{22}\frac{\partial w}{\partial x}\frac{\partial^2 w}{\partial x^2}+B_{22}\frac{\partial v}{\partial x}\frac{\partial^2 v}{\partial x^2}+D_{22}\frac{\partial^2 \varphi_y}{\partial x^2}\right)-\frac{8}{15}l_1^2 A_{22}\varphi_y \tag{A45}$$

$$M^{2}_{zzx}=\int_s \tau^{(1)}_{zzx} y dA=-\frac{2}{5}l_1^2\left(C_{22}\frac{\partial^2 u}{\partial x^2}+\frac{1}{R}C_{22}\frac{\partial w}{\partial x}+C_{22}\frac{\partial w}{\partial x}\frac{\partial^2 w}{\partial x^2}+C_{22}\frac{\partial v}{\partial x}\frac{\partial^2 v}{\partial x^2}+F_{22}\left(\frac{1}{R}\frac{\partial \varphi_x}{\partial x}-\frac{\partial^2 \varphi_z}{\partial x^2}\right)\right)-\frac{8}{15}l_1^2 C_{22}\varphi_y \tag{A46}$$

$$T_{zzy}=\int_s \tau^{(1)}_{zzy} dA=-\frac{2}{15}l_1^2\left(A_{22}\frac{\varphi_x}{R}+A_{22}\frac{\partial^2 v}{\partial x^2}-2A_{22}\frac{\partial \varphi_z}{\partial x}-B_{22}\frac{\partial^2 \varphi_x}{\partial x^2}\right) \tag{A47}$$

$$M^{1}_{zzy}=\int_s \tau^{(1)}_{zzy} z dA=-\frac{2}{15}l_1^2\left(B_{22}\frac{\varphi_x}{R}+B_{22}\frac{\partial^2 v}{\partial x^2}-2B_{22}\frac{\partial \varphi_z}{\partial x}-D_{22}\frac{\partial^2 \varphi_x}{\partial x^2}\right) \tag{A48}$$

where

$$\begin{aligned}&\left(A_{11},B_{11},C_{11},D_{11},F_{11}\right)=\int_A Q_{11}\left(1,\mathrm{z},\mathrm{y},\mathrm{z}^2,y^2\right)dA,\\&\left(\tilde{A}_{11},\tilde{B}_{11},\tilde{C}_{11}\right)=\int_A \alpha_{xx}Q_{11}\left(1,\mathrm{z},\mathrm{y}\right)dA,\\&\left(A_{22},B_{22},C_{22},D_{22},F_{22}\right)=\int_A Q_{22}\left(1,\mathrm{z},\mathrm{y},\mathrm{z}^2,y^2\right)dA,\end{aligned} \tag{A49}$$